BERLIN 2022

IWCGT–8

ABSTRACT BOOK

8th International Workshop on Crystal Growth Technology

May 29 – June 2, 2022

Berlin | Germany

We thank our sponsors and exhibitors for their valuable support:

PVA TePla
Crystal Growing Systems

BAMAC®
Bamac-electric GmbH

STR
SOFTWARE AND CONSULTING SERVICES
FOR MODELING OF BULK CRYSTAL GROWTH,
EPITAXY AND SEMICONDUCTOR DEVICES

SCIDRE
SCIENTIFIC INSTRUMENTS DRESDEN GMBH

Freiberg Instruments

DFG Deutsche Forschungsgemeinschaft
German Research Foundation

The workshop is conducted under the auspices of:

International Organisation for Crystal Growth (IOCG)
Deutsche Gesellschaft für Kristallwachstum und Kristallzüchtung e.V. (DGKK)

IWCGT–8

8th International Workshop on Crystal Growth Technology

29 May–2 June 2022 | Berlin (Germany)

Organized by
LEIBNIZ-INSTITUT FÜR KRISTALLZÜCHTUNG
im Forschungsverbund Berlin e.V.

Opening Message

Crystal growth will remain utmost important, continuing to shape the foundation of major advances in technology. The International Workshop series IWCGT – initiated by Hans Scheel in 1998 – is devoted to crystal growth technology, which also covers industrial scale technologies and equipment. The focus lies on the preparation of bulk and substrate crystals. The workshop aims to provide links between R & D and actual production, bridging science and practice.

The IWCGT-8, originally scheduled for June 2020, had to be postponed to 2022 due to the worldwide COVID pandemic. In addition to scientific exchange, the IWCGT has the objective of promoting communication and cooperation among crystal growth technologists. Our community lives from personal meetings and discussions. Therefore, we did not want to switch to a virtual format.

We are very pleased with the active support we have received during planning and organization, and we especially appreciate your participation! We thank all lecturers, international experts that will present a detailed overview on different aspects on current crystal growth technology. We also thank the attendees that present their research at the evening poster sessions. Last but not least, we thank our sponsors and exhibitors (see second cover page and the advertisements in the booklet), whose commitment helped to make this meeting possible.

We wish you a pleasant and informative workshop! Please observe any hygiene instructions that might be in place at the time of the workshop. Stay healthy!

Matthias Bickermann

R. Radhakrishnan Sumathi

Christiane Frank-Rotsch

IWCGT-8 Invited Lecturers

Rafael Dalmau, Hexatech (USA)

Natascha Dropka, IKZ Berlin (Germany)

Stefan Eichler, Freiberger Compound Materials (Germany)

Yasunori Furukawa (古川保典), Oxide Corp. (Japan)

Jan Havlíček, Crytur (Czech Rep.)

Christian Hell, Hellma IV IR Photonics (Germany)

Andriy Hikavyy, IMEC (Belgium)

Patricia Jeandel, Cristal Innov (France)

Christian Kranert, Fraunhofer IISB+THM (Germany)

Zhixin Li (黎志欣), Linton Machine (China)

Robert Menzel, IKZ Berlin (Germany)

Andreas Mühe, PVA TePla (Germany)

Yohei Otoki (乙木 洋平), SCIOCS (Japan)

P.S. Raghavan, OnSemi (USA)

Peter Rudolph, Crystal Growth Consulting (Germany)

Shashwati Sen, Bhabha Atomic Research Centre (India)

Ludwig Stockmeier, Siltronic (Germany)

Anton Tremsin, University of California, Berkeley (USA)

Martin Wegener, Karlsruhe Inst. of Technology (Germany)

Yadong Xu (徐亚东), Northwestern Polytechnical Univ. (China)

Kader Zaidat, SiMAP INP Grenoble (France)

Workshop Location

Pentahotel Berlin-Köpenick, Grünauer Str. 1, 12557 Berlin, phone +49-30-654790
Parking garage is available for a fee, south of the hotel entrance

Excursion and Dinner (June 1)

Boat tour from/landing stage “Köpenick/Luisenhain”

Dinner at the “Ratskeller Köpenick”
Alt Köpenick 21, 12555 Berlin, phone +49-30-6555178

Public Transport

From Berlin Main Railway Station:
use local train S3 to “Köpenick” (12 stops),
then Tram 63, 68 or Bus 164 to “Köllnischer Platz” (4 stops)

or local train S9 to “Adlershof” (12 stops), further as below

From Berlin-Brandenburg Airport:
use local trains S45 or S9 to “Adlershof” (5 stops), then Tram 61, 63 or Bus 164 to “Köllnischer Platz” (5 stops)

IWCGT-8 Organizers

Matthias Bickermann, IKZ Berlin (Germany) (Chair)

R. Radhakrishnan Sumathi, IKZ Berlin (Germany) (Co-Chair)

Christiane Frank-Rotsch, IKZ Berlin Germany (Co-Chair)

IWCGT Steering Committee

Matthias Bickermann, IKZ Berlin (Germany)

Edith D. Bourret-Courchesne, LBNL (USA)

Mitch Chou, National Sun Yat-Sen Univ. (Taiwan)

Hanna Dabkowska, McMaster Univ. (Canada)

Ben Depuydt, Umicore (Belgium)

Jeffrey J. Derby, Univ. Minnesota (USA)

Thierry Duffar, INP Grenoble (France)

Roberto Fornari, Univ. Parma (Italy)

Vincent J. Fratello, Integrated Photonics Inc. (USA)

Jochen Friedrich, Fraunhofer IISB (Germany)

Alexander Gektin, Inst. Single Crystals, Kharkov (Ukraine)

Koichi Kakimoto, Tohoku Univ. (Japan)

Frank M. Kießling, IKZ Berlin (Germany)

Chung-Wen Lan, National Taiwan Univ. (Taiwan)

Yusuke Mori, Osaka Univ. (Japan)

Maria Porrini, former MEMC/GlobalSemi (Italy)

Hans J. Scheel (Switzerland)

Peter G. Schunemann, BAE Systems (USA)

Deren Yang, State Key Lab., Zhejiang Univ. (China)

Evgeny V. Zharikov, General Phys. Inst., Moscow (Russia)

Sunday, May 29, 2022

04:00 pm Registration
(Front Desk, Conference area, Pentahotel Köpenick)

05:00 pm Welcome

06:30 pm Dinner

07:30 pm Get together

08:00 pm **Panel Discussion:** Struggling with pandemic and war.
Panelists to be announced

Monday, May 30, 2022

08:50 am Welcome

09:00 am **Is the Cold Crucible Adapted for Single Crystal Growth?**

Kader Zaidat[1], Samah Alradi[1], Hamza Abouchi[1], Florin Baltaretu[2], Xuefeng Han[1], Mahmoud Alradi[1], Christian Garnier[1], Ghatfan Hasan[1], Roland Ernst[1], Abdeldjellil Nehari[4], Kheirreddine Lebbou[4], Abdellah Kharicha[3]

[1]Univ. Grenoble Alpes, SIMAP, Grenoble, France; [2]Technical University of Civil Engineering Bucharest, Romania; [3]Christian-Doppler Laboratory for Metallurgical Applications of Magnetohydrodnamics, Leobben, Austria; [4]Institut Lumière Matière, UMR5306 Université Lyon1-CNRS, Villeurbanne, France;
kader.zaidat@simap.grenoble-inp.fr

09:50 am **Growth Ridge Analysis - A Smart Tool to Investigate Cz Processes and Crystals**

Christian Kranert[1,2], Thomas Jung[2], Georg Raming[3], Alfred Miller[3], Christian Reimann[2,1], Jochen Friedrich[2,1]

[1]Fraunhofer THM, Freiberg, Germany; [2]Fraunhofer IISB, Erlangen, Germany; [3]Siltronic AG, Burghausen, Germany; christian.kranert@iisb.fraunhofer.de

10:40 am Coffee break

11:10 am **Growth of Silicon Crystals Using a Self-Crucible Concept**

Robert Menzel, Kaspars Dadzis, Frank M. Kießling, Nikolai Lorenz-Meyer, Benedikt Faraji-Tajrishi, Angelina Nikiforova, Nikolay Abrosimov, Helge Riemann

Leibniz-Institut für Kristallzüchtung (IKZ), Berlin, Germany;
robert.menzel@ikz-berlin.de

12:00 pm Break

12:30 pm Lunch

02:10 pm **Venture Business in Photonics: A Long Road from Start-up to IPO, and Outlook**

Yasunori Furukawa
Oxide Corporation, Yamanashi, Japan; furukawa@opt-oxide.com

03:00 pm **In-Situ Crystal Growth Diagnostic Using Energy-Resolved Neutron Imaging** (ONLINE)

Anton Tremsin
University of California at Berkeley, United States of America; astr@berkeley.edu

03:50 pm Coffee Break

04:30 pm **Growth of Large Diameter Yttrium Aluminium Garnet Crystals by Czochralski Method**

Jan Polák, Jan Havlíček, Karel Bartoš, Jindřich Houžvička
Crytur, spol. s r.o., Turnov, Czech Republic; jan.havlicek@crytur.cz

05:20 pm **Challenges in the Growth of Large Size Scintillator Single Crystal**

Shashwati Sen Yeram, B. Tiwari, M. Tyagi, S.G. Singh, D.G. Desai, M. Ghosh, S. Pitale, G.D. Patra, A.K. Singh
Bhabha Atomic Research Centre, Mumbai, India; shash@barc.gov.in

06:30 pm Dinner

07:30 pm **Poster Session** (Program see below)

Tuesday, May 31, 2022

08:50 am Welcome

09:00 am **Formation of Secondary Phase Particles and the Interplay Mechanism with Extended Dislocations in CdZnTe Bulk Crystals** (ONLINE)

Yadong Xu
Northwestern Polytechnical University, Xi'an, China; xyd220@nwpu.edu.cn

09:50 am **Growth Specifics Of CdTe And Related Mixed Systems**

Peter Rudolph
Crystal Technology Consulting, Schönefeld, Germany; rudolph@ctc-berlin.de

10:40 am Break

11:10 am **Recent Topics of High Quality VAS-GaN Substrates for Realizing High Performance of Opto/electric Devices in Mass Production (ONLINE**

Yohei Otoki
Sumitomo Chemical SCIOCS, Hitachi, Japan; otokiy@sc.sumitomo-chem.co.jp

12:00 pm Break

12:30 pm Lunch

02:10 pm **3D Metamaterials – Rationally Designed Artificial Crystals**

Martin Wegener
Karlsruhe Institute of Technology (KIT), Germany; martin.wegener@kit.edu

03:00 pm **UV-C Transparent PVT AlN Substrates** (ONLINE)
Rafael Dalmau, Samuel Kirby, Jeffrey Britt, Raoul Schlesser
HexaTech, Inc., Morrisville, United States of America; rdalmau@hexatechinc.com

03:50 pm Break

04:30 pm Properties of State-of-the-Art Laser Grade GaAs Substrates
Stefan Eichler
Freiberger Compound Materials, Freiberg, Germany; stefan.eichler@freiberger.com

05:20 pm **Evolution of Silicon Carbide Substrate Production/Understanding and Managing Defects in Silicon Carbide**
Santhanaraghavan Parthasarathy
ON Semiconductor, Phoenix, United States of America; raghavan@onsemi.com

06:30 pm Dinner

07:30 pm **Poster Session** (Program see below)

Wednesday, June 1, 2022

08:50 am Welcome

09:00 am **Can Machine Learning Help Us Grow Advanced Crystals?**
Natasha Dropka[1], Martin Holena[2]
[1]Leibniz-Institut für Kristallzüchtung (IKZ), Berlin, Germany; [2]Leibniz Institute for Catalysis (LIKAT), Rostock, Germany; natascha.dropka@ikz-berlin.de

09:50 am **Big Data From Industrial Czochralski Silicon**
Ludwig Stockmeier[1], Georg Raming[2]
[1]Siltronic AG, Freiberg, Germany; [2]Siltronic AG, Burghausen, Germany; ludwig.stockmeier@siltronic.com

10:40 am Break

11:10 am **A short view on optical properties of CZ grown Germanium Crystals**
Christian Hell
Hellma Material IV IR Optics, Eisenach, Germany; christian.hell@iv-ir-optics.com

12:00 pm **Low Temperature Epitaxial Growth of Group IV Materials in View of Electrical Device Applications**
Andriy Yakovitch Hikavyy, Roger Loo, Clement Porret, Gianluca Rengo, Erik Rosseel, Robert Langer
imec, Leuven, Belgium; Andriy.Hikavyy@imec.be

12:50 pm Lunch

02:00 pm Break (and Steering Committee Meeting)

03:50 pm **Boat Tour** "Müggelsee"
(Please come to the landing stage, see map)

06:15 pm **Workshop Dinner**, "Ratskeller Köpenick"
(We meet in the Hotel Lobby to walk there)

Thursday, June 2, 2022

08:50 am Welcome

09:00 am **Crystal Growth R&D and Technology : For a more competitive European community**

Patricia Jeandel
Crystal Innov, Villeurbanne, France; patricia.jeandel@cristalinnov.com

09:50 am **Recent Progress in Silicon Crystal Growth Technology for Solar Industry**

Zhixin Li
Linton Technologies Group, Dalian, China; lizx@lintonmachine.com

10:40 am Break

11:10 pm **Tools for the Industrial Production of Defect Controlled Silicon Ingots**

Andreas Mühe[1], Alexey Denisov[1], Frank Mosel[1], Tse Wei Lu[2], Feng Hou Kun[2]
[1]PVA TePla AG, Wettenberg, Germany; [2]XuZhou XinJing Semiconductor Technology Co. Ltd., China; andreas.muehe@pvatepla.com

12:00 pm Closing Ceremony

12:30 pm Lunch

Poster Session

Posters are on display throughout Monday to Wednesday; all posters are presented Monday and Tuesday 07:30 pm-09:30 pm.

P01 **Luminescence Study Of Trivalent Erbium Ions Doped Into Fluoride Crystals Grown By Bridgman Method**

Gabriel Buse, Marius Stef, Andrei Racu, Irina Nicoara, Daniel Vizman
West University of Timisoara, Romania; gabriel.buse@e-uvt.ro

P02 **Self-learning Crystal Growth Furnaces: Perspective for Artificial Intelligence Technologies**

Kaspars Dadzis, Arved Enders-Seidlitz, Iason Tsiapkinis
Leibniz-Institut für Kristallzüchtung (IKZ), Berlin, Germany; kaspars.dadzis@ikz-berlin.de

P03 **Analysis of Bubble Engulfment During Melt Crystal Growth**

Swanad Pawar, Jeffrey J. Derby
University of Minnesota, United States of America; derby@umn.edu

P04 **Analysis of Single-Crystal Diamond Growth Via HPHT**

Scott S. Dossa[1], Ilya Ponomarev[2], Boris Feigelson[3], Marc Hainke[4,5], Christian Kranert[5], Jochen Friedrich[5], Jeffrey J. Derby[1]
[1]University of Minnesota, United States of America; [2]Euclid Beamlabs, LLC, United States of America; [3]U.S. Naval Research Laboratory, United States of America; [4]Ostbayerische Technische Hochschule, Amberg-Weiden, Germany; [5]Fraunhofer IISB, Erlangen, Germany; doss0032@umn.edu

P05 **Solidification of the Large Diameter Uniform Sb doped Germanium Crystals**

Michael Gonik[1], Florin Baltaretu[2]
[1]CM "Photon"; [2]Technical University of Civil Engineering, Bucharest, Romania; michael.a.gonik@gmail.com

P06 **Crystal Growth of the Large-scale Semiconductor Crystals by the Modified Cz Method**

Michael Gonik[1], Florin Baltaretu[2]
[1]CM "Photon"; [2]Technical University of Civil Engineering, Bucharest, Romania; michael.a.gonik@gmail.com

P07 **Revisiting the Growth of Large (Mg,Zr):$SrGa_{12}O_{19}$ Single Crystals: Core Formation and Its Impact on Structural Homogeneity Revealed by Correlative X-ray Imaging**

Christo Guguschev[1], Carsten Richter[1], Mario Brützam[1], Kaspars Dadzis[1], Christian Hirschle[2], Thorsten M. Gesing[3,4], Michael Schulze[1], Albert Kwasniewski[1], Jürgen Schreuer[2], Darrell G. Schlom[5,6,1]

[1]Leibniz-Institut für Kristallzüchtung (IKZ), Berlin, Germany; [2]Institut für Geologie, Mineralogie und Geophysik, Ruhr-Universität Bochum, Bochum, Germany; [3]University of Bremen, Institute of Inorganic Chemistry and Crystallography, Bremen, Germany; [4]MAPEX Center for Materials and Processes, Bremen, Germany; [5]Department of Materials Science and Engineering, Cornell University, Ithaca, United States; [6]Kavli Institute at Cornell for Nanoscale Science, Ithaca, United States; christo.guguschev@ikz-berlin.de

P08 **Growth of high quality CdZnTe bulk crystals using the Vertical Gradient Freeze technique**

Timotée Journot

CEA Leti, Grenoble, France; timotee.journot@cea.fr

P09 **Epitaxial Growth of III-V Semiconductors on Silicon: Critical Impact of the Si Substrate**

Maud Jullien, Tony Rohel, Karine Tavernier, Antoine Létoublon, Rozenn Bernard, Olivier Durand, Yoan Leger, Nicolas Bertru, Charles Cornet

Institut FOTON, INSA Rennes, France; maud.jullien@insa-rennes.fr

P10 **Growth of 6N Purity Germanium Single Crystal Using Czochralski Technique**

Giri Dhari Patra, S G Singh, M Ghosh, S Pitale, A Singh, S Sen, L M Pant

Bhabha Atomic Research Centre, Mumbai, India; gdpatra@barc.gov.in

P11 **Crystal growth, Morphology, and Luminescence Properties of LuSAG:Tm Single Crystals**

Jan Pejchal[1], Jan Havlíček[1,2], Jan Šulc[3], Karel Nejezchleb[2], Helena Jelínková[3]

[1]Institute of Physics AS CR, Prague, Czech Republic; [2]Crytur, spol. s r.o., Turnov, Czech Republic; [3]Faculty of Nuclear Sciences and Physical Engineering, Czech Technical University, Prague, Czech Republic; jan.havlicek@crytur.cz

P12 **Numerical Study Of Dislocation Density Distribution In Silicon Crystals Under Different Temperature Conditions**

Andrejs Sabanskis[1], Kaspars Dadzis[2], Lucas Vieira[2], Robert Menzel[2], Janis Virbulis[1]

[1]Institute of Numerical Modelling, University of Latvia, Riga, Latvia; [2]Leibniz-Institut für Kristallzüchtung (IKZ), Berlin, Germany; andrejs.sabanskis@lu.lv

P13 **High Energy Computed Tomography as a Tool for Validation of Numerical Simulations of Ammonothermal Crystal Growth of GaN**

Saskia Schimmel[1], Michael Salamon[2], Daisuke Tomida[3], Tohru Ishiguro[4], Yoshio Honda[3], Shigefusa F. Chichibu[3,4], Hiroshi Amano[3]

[1]Friedrich-Alexander-Universität Erlangen-Nürnberg, Crystals Growth Lab, Materials for Electronics and Energy Technology (i-MEET), Erlangen, Germany; [2]Fraunhofer Institute for Integrated Circuits IIS, Division Development Center X-Ray Technology, Fürth, Germany; [3]Institute of Materials and Systems for Sustainability, Nagoya University, Nagoya, Japan; [4]Institute of Multidisciplinary Research for Advanced Materials, Tohoku University, Sendai, Japan; saskia.schimmel@fau.de

P14 **Effect of Co-Doping in the Growth and Scintillation Performance of $CeBr_3$**

Durgesh Singh Sisodiya, Shiv Govind Singh, Giri Dhari Patra, Shashwati Sen
Bhabha Atomic Research Centre, Mumbai, India; dsinghsisodiya1996@gmail.com

P15 **Growth, Structural and Optical Properties of $Gd_2Ti_2O_7$ Single Crystals**

Suganya Murali[1], Ganesan K[2], Vijayakumar P[2], Amirdha Sher Gill[3], Sarguna R[2], Edward Prabu A[2], Moorthybabu S[1], Ganesamoorthy S[2]
[1]Crystal Growth Center, Anna University, Chennai, India; [2]Materials Science Group, Indira Gandhi Center for Atomic Research, Kalpakkam, India; [3]Sathyabama Institute of Science and Technology, Chennai, India; suganyatvmalai29@gmail.com

P16 **Investigations on n-Type Doping on OFZ Grown Beta-Gallium Oxide Single Crystals for Power Device Applications**

Ananthu Vijayan V L, Kaza Venkata Akshita, Dhandapani Dhanabalan, Rajendran Hariharan, Sridharan Moorthy Babu
Crystal Growth Center, Anna University, Chennai, India; anugwri@gmail.com

P17 **Growth and Characterization of $Tb_3Ga_5O_{12}$ Single Crystals**

Miki Watanabe[1,2], Takeshi Hayashi[1], Yutaka Anzai[1], Isao Tanaka[2]
[1]Oxide Corporation; Yamanashi, Japan, [2]University of Yamanashi, Japan;
miki.watanabe@opt-oxide.com

P18 **In-band Pumped Ho:CALGO Crystal For Efficient High-power Laser Operation at 2.1 µm**

Weichao Yao[1], Yicheng Wang[1], Christoph Liebald[2], Daniel Rytz[2], Volker Wesemann[2], Klaus Dupré[2], Daniel Dümichen[2], Tamara Berzen[2], Mark Peltz[2], Clara J. Saraceno[1]
[1]Ruhr-Universität Bochum, Germany; [2]Electro-Optics Technology GmbH, Germany;
weichao.yao@ruhr-uni-bochum.de

P19 **Solid-State Microwave Generators at 2.45 GHz for Microwave Plasma Assisted CVD and ALD Processes**

Gerd Hartmut Hintz
TRUMPF HÜTTINGER, Germany; gerd.hintz@trumpf.com

P20 **Advanced Modeling of Melt Turbulence, Impurities and Bubble Transport in Cz Silicon Crystal Growth**

Vladimir Artemyev, Andrey Smirnov
Semiconductor Technology Research d.o.o., Beograd, Serbia;
vladimir.artemyev@str-soft.com

P21 **Digital Defect Traceability across Sapphire Processing: Case Study on Micro-LED Chain**

Ivan Orlov[1], Gourav Sen[2], Caroline Chèze[1], Frédéric Falise[1]
[1]Scientific Visual, Lausanne, Switzerland, [2]Fametec-Ebner GmbH, Leonding, Austria;
welcome@scientificvisual.ch

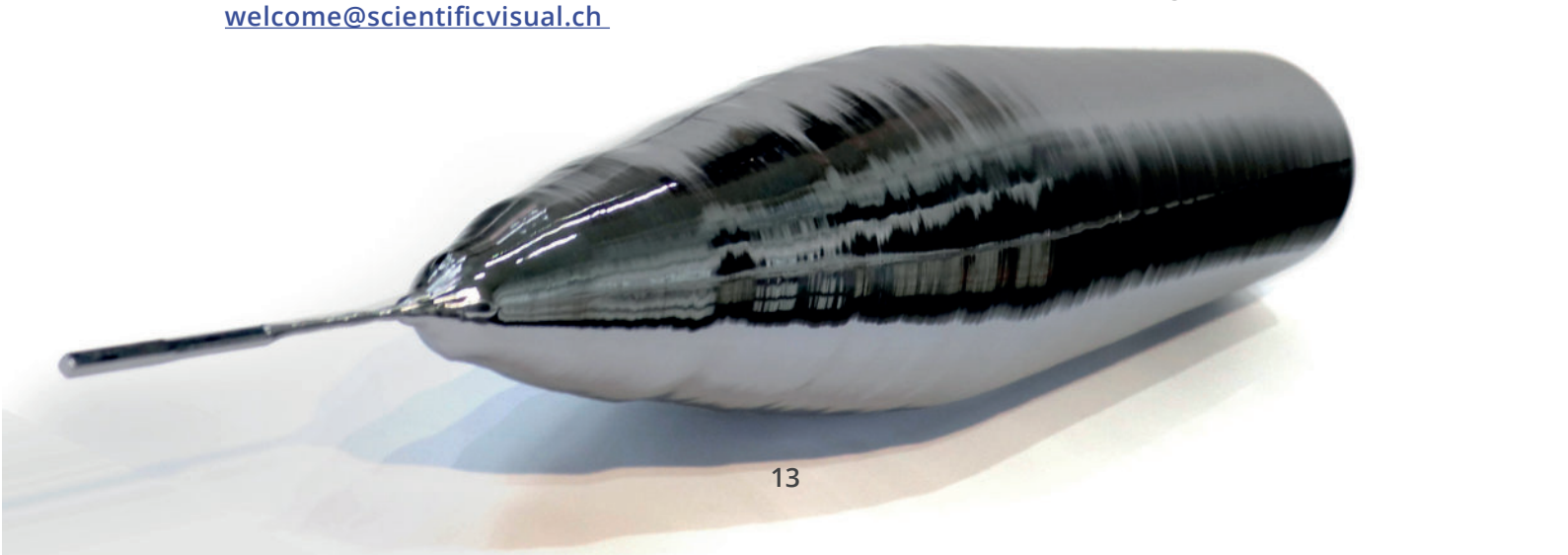

DRESDEN MATERIALS

An accessible joint lab for crystal growth and materials research

State-of-the-art equipment for sample preparation, crystal growth and sample analysis available for rental usage in Dresden

Synthesis and Crystal Growth

Sample Preparation → **Sample Analysis**

Reserve time slots and make your experiment with our technical support
Save your money and lab space by renting instead of purchasing
Collaborative on-demand access to cutting-edge equipment
"Remote experiment" option to safe travel time and costs
Test new parameters for your samples and processes

Example equipment:

A-HSO – Advanced High Pressure Oxygen Furnace (200 bar O_2)

HKZ – High Pressure High Temperature Optical Floating Zone Furnace

LKZ – High Temperature Laser Floating Zone Furnace

Please contact us for details and reservations:
E-mail: info@dresden-materials.de
Phone: +49 (0) 351 8422 1467

www.dresden-materials.de

A cooperation of ScIDre GmbH and IFW Dresden

ScIDre Scientific Instruments Dresden GmbH

IFW Leibniz Institute for Solid State and Materials Research Dresden

Monday, May 30, 2022

LECTURES

Is the cold crucible adapted for single crystal growth?

K. Zaidat[1], S. Al-Radi[1,2], H. Abouchi[2], Fl. Baltaretu[3], X. Han[1], M. Al-Radi[1,2], C. Garnier[2], G. Hasan[2], R. Ernst[2], A. Nehari[4], K. Lebbou[4] and A. Kharicha[5],

[1]Univ. Grenoble Alpes, SIMAP, F-38000 Grenoble, France
[2]CNRS, SIMAP, F-38000 Grenoble, France
[3]Technical University of Civil Engineering Bucharest, Romania
[4] Institut Lumière Matière, UMR5306 Université Lyon1-CNRS, Université de Lyon, Lyon 69622, Villeurbanne Cedex, France
[5] Christian-Doppler Laboratory for Metallurgical Applications of Magnetohydrodnamics, Leobben, Austria

kader.zaidat@simap.grenoble-inp.fr

Abstract:

Currently in the semiconductor industry more than 90% of silicon crystals are grown by the Czochralski (Cz) and Floating zone (FZ) method. In the Cz method, fused silica (SiO_2) crucibles and graphite heaters are used inside furnaces. The surface of the crucibles, which are in contact with the molten silicon, is gradually dissolved into the melt [1]. This reaction occurs during all the crystal growth process contributes to the presence of oxygen in silicon crystals and has a lot of consequence in the crystal quality (OSF, dislocation, precipitation of impurities…).

In the eighties, Wenkus & Menashi [2] and Ciszek [3] used a cold crucible in order to decrease the oxygen contamination level. They have shown that it was possible to get a small single crystal (2.5 cm in diameter) with a very low oxygen contamination. They concluded also that one of the major problems, as yet unresolved in the use of the cold crucible for the growth of single crystals, is related to the stabilization and precise control of the melt flow.

In this presentation, we will present the state of the art on the crystal growth in a cold crucible and we will present a new generation of cold crucible [4] in order to stabilize the fluid flow induced by the Lorentz force inside the melt.

References:

1: K. Kakimoto, B. Gao, X. Liu, S. Nakano, Growth of semiconductor silicon crystals, *Progress in Crystal Growth and Characterization of Materials* 62 (2016), 273–285.

2: J.F. Wenckus, W.P. Menashi: Growth of High Purity Oxygen-Free Silicon by Cold Crucible Techniques, *Report of the US Air Force*, RADC-TR-82-171 (1980).

3: T.F. Ciszek, Growth and Properties of (100) and (111) dislocation free silicon crystals from a cold crucible, *Journal of Crystal Growth* 70 (1984), 324-329.

4: K. Zaidat, C. Garnier et G. Hasan, New cold crucible, Patent WO/2020/161269 (2020)

Growth ridge analysis – a smart tool to investigate Cz processes and crystals

Christian Kranert[1,2,*], Thomas Jung[2], Georg Raming[3], Alfred Miller[3], Christian Reimann[2,1], Jochen Friedrich[2,1]
[1]Fraunhofer THM, Am St.-Niclas-Schacht 13, 09599 Freiberg, Germany
[2]Fraunhofer IISB, Schottkystraße 10, 91058 Erlangen, Germany
[3]Siltronic AG, Rudolf-Hess-Straße 24, 84489 Burghausen, Germany
*christian.kranert@iisb.fraunhofer.de

Crystals are inherently anisotropic and thus exhibit orientation-dependent properties. In particular, during crystallization from melt, certain crystal planes may grow as atomically smooth surfaces while other interfaces are rough. This has several consequences on both the growth and the properties of the crystal: The nucleation on the smooth interface requires a certain melt supercooling. In the case of edge facets, this supercooling is the cause for melt transfer towards the growth ridge which affects the crystal shape on a wide scale [1,2] and may cause particles to be transported towards the interface causing dislocations and twinning [3]. Further, facets are known to be the cause of twinning also in the absence of particles, especially in III-V semiconductors, and to result in a locally different effective segregation coefficient [4]. They are also suspected to be an important origin of dislocation formation in highly doped silicon [5]. Thus, despite the facets only covering a marginal fraction of the crystal cross section, they can be highly relevant for the industrial crystal production. Finally, for crystals grown without contact to a crucible, e.g. by the Czochralski (Cz) or float zone (FZ) approach, the presence of edge facets typically causes protrusions on the surface of a crystal body – the growth ridges.

It is a common procedure to monitor the growth ridge for disappearance during crystal growth in order to timely detect dislocation formation and remelt the dislocated crystal part. However, the growth ridge geometry has not yet been a serious object of investigation despite extensive theoretical work by Voronkov from already decades ago [6]. In this presentation, we will introduce our experimental approach to measure the growth ridge geometry by optical profilometry. This fast and non-destructive technique yields not only comprehensive information on the facet properties with a high resolution in growth direction, but also on the thermal conditions in the vicinity of the three-phase line.

Two kinds of information can be deduced from these measurements: First, based on the comprehensive, high-resolution data, models for the facet growth and growth ridge geometry can be verified and refined. Specifically, we can confirm that the growth ridge geometry of Cz silicon is in very good agreement to Voronkov's theory [2,6]. However, this theory is limited to stationary conditions which are in general not present during an actual crystal growth process due to diameter fluctuations, pulling rate adjustments, melt convection and crystal rotation. We developed a simple model which explains the impact of these conditions on the facet and growth ridge and gives additional insights on the processes at the edge facet. Second, we extract information from the data which are useful for the process evaluation and development. For example, the temperature gradient at the crystal surface can be calculated from the growth ridge geometry and it may be used as an early warning sign for the occurrence of crystal twisting.

[1] Krauze et al., J. Cryst. Growth 520, 68 – 71 (2019), doi: 10.1016/j.jcrysgro.2019.04.030
[2] Stockmeier et al., J. Crys. Growth 515, 26 – 31 (2019), doi: 10.1016/j.jcrysgro.2019.03.009
[3] Kearns: Origin of Growth Twins during Czochralski Growth of Heavily Doped, Dislocation-Free Single Crystal Silicon. PhD thesis (2019)
[4] Chen et al., J. Crys. Growth 103, 243 – 250 (1990), doi: 10.1016/0022-0248(90)90195-Q
[5] Stockmeier et al., Cryst. Res. Technol. 46, 1600373 (2017), doi: 10.1002/crat.201600373
[6] Voronkov, Izvest. Akad. Nauk. SSSR, Ser. Fiz. 47, 210 – 218 (1983)

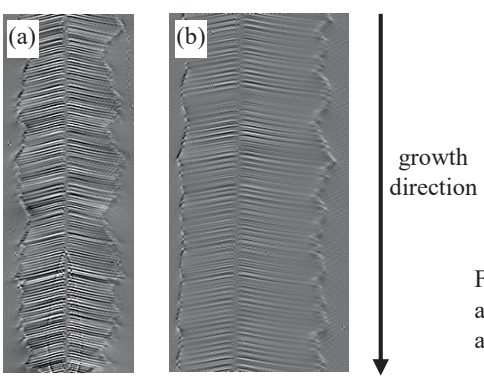

Fig. 1 Growth ridge of Cz silicon crystals, a) with fluctuating size and b) with strongly asymmetric shape. Both effects are results of the non-stationary conditions during actual crystal growth processes.

Growth of silicon crystals using a self-crucible concept

R. Menzel, K. Dadzis, Frank M. Kießling, N. Lorenz-Meyer, B. Faraji-Tajrishi, A. Nikiforova, N. Abrosimov and H. Riemann

Leibniz-Institut für Kristallzüchtung (IKZ), Max-Born-Str. 2, 12489 Berlin, Germany

The Silicon Granulate Crucible (Si-GC) method [1] is a "self-crucible" crystal growth concept (Fig: left), with the potential to combine the advantages of the established production methods for high-purity crystalline Si, needed e.g. for power devices or high-efficiency solar cells. Similar to the Floating-Zone (FZ) process for Si and in contrast to the Czochralski (Cz) method and its further developments like Magnetic Czochralski (MCz), the crystal is not contaminated during growth. In the Si-GC method, the melt is not contaminated due to the use of a quartz crucible or graphite heaters as in Cz. Consequently, no impurities like O, C or transition metals are incorporated in the crystal, which would deteriorate the device performance. A cost-efficient production would be possible due to the use of low-cost fluidized bed granules as Si raw material, an energy efficient continuous process using inductive heating and practically no consumables. Furthermore, the achievable diameter of the crystal is not limited by a feed rod as in FZ.

In the three-year research project Silizium Granulat Eigentiegelverfahren (SiGrEt), funded by the Leibniz Association (Leibniz-Wettbewerb 2016) and carried out at the IKZ, the feasibility of the Si-GC process was demonstrated. The main findings of the project and crystal growth results will be presented and evaluated with regard to the further development of the Si-GC process, towards an industrial production method. A laboratory set-up (Fig1: mid) was developed, using a modified Steremat FZ1505 crystal growth machine. A special starting technique using a susceptor was applied that allowed to generate a large melt pool, followed by seeding with the Dash method and defined growth of the crystal shoulder. It was found that the Si-GC process is self-stabilizing in the cylindrical growth phase but maintaining a constant melt pool filling level is critical here. It will be elaborated on the complex interplay of process parameters on the growth conditions by means of a lumped parameter model, which was developed for the Si-GC process [2].

For solar cells based on crystalline Si, n-type mono is predicted to be the dominating base material by the year 2029 [3] In the Si-GC process (Fig: right), which is continuously replenished with raw material, a homogeneous axial dopant profile can be achieved via gas phase doping, even for n-type using phosphine. Gas phase doping using phosphine or diborane was successfully applied in the growth experiments. The resistivity measurements conducted on grown material showed that a homogeneous axial dopant profile can be achieved but precise initial doping of the large melt pool is needed for better results. Furthermore, the achieved purity in the grown Si-GC crystals was investigated [4]. FTIR measurements showed a low O concentration below the detection limit of $1 \cdot 10^{16}$ a/cm^3, which is at the level of FZ-Si. The carbon concentration of $5 \cdot 10^{16}$ a/cm^3 was higher than usually found in FZ-Si. ICP-MS measurements conducted at the Fraunhofer CSP Halle showed a concentration below 10^{15} a/cm^3 of every other investigated impurity as e.g. Al, Ti, Fe, Ni and Cu. A comparison with impurity measurements on the raw material indicated, that all measured impurities were already present in the raw material and not incorporated during crystal growth. Hence, for growth of crystals with higher purity, raw material with higher purity should be used, e.g. electronic grade chunks/chips.

To investigate a possible upscaling of the SI-GC process, crystals with a diameter of up to 4 inch were successfully grown. However, here the growth rate was limited to avoid contact of unmolten granular particles with the triple-phase line. For growth of crystals with even larger diameter, not solid but liquid Si replenishment to the melt pool may be needed.

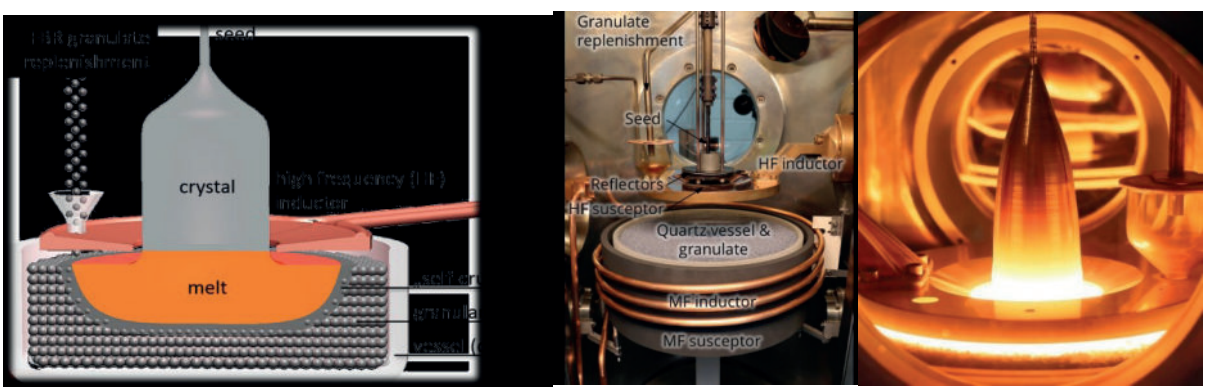

Fig: left: Si-GC growth concept, mid: growth setup, right: 2-inch Si-GC crystal during growth

[1] H. Riemann et al.; International Patent, WO2011063795 A1, (2011).
[2] M.N.L. Lorenz-Meyer et al.; DOI: 10.1002/crat.202000044 (2020).
[3] ITPRV Report 2022; https://www.vdma.org/international-technology-roadmap-photovoltaic.
[4] K. Dadzis et al.; DOI: 10.1007/s11664-020-08309-1.

Venture Business in Photonics: A Long Road from Start-up to IPO, and Outlook

Oxide Corporation, Yasunori Furukawa

E-mail: furukawa@opt-oxide.com

While there are so many great results coming out of national research labs in Japan, they are less utilized compared to those in the US and Europe. I started Oxide Corporation in 2000, aiming at returning the fruition of fundamental research to society. It was a big decision to start a company in those days, leaving a stable job as a government employee, and I had much hesitation. However, words from my former advisor at Stanford University, where I studied in 1992, pushed me through; "The biggest risk in life is taking none."

I started the company with a big ambition to commercialize stoichiometric $LiNbO_3$ and $LiTaO_3$ crystals grown by the double crucible CZ method, but the reality was far from ideal. It sounded nice to be a venture business spinning off from a national lab. But in practice, I knew nothing about running a company, which was just 3 people in a prefab shed. Moreover, the target markets for the stoichiometric $LiNbO_3$ and $LiTaO_3$ crystals, QPM-SHG device for Blu-Ray, and holographic storage were both overcome by well-known competing technologies such as blue LD. Opportunities were just gone, and we faced the risk of going out of business. The business environment worsened, and despair was looming, when NTT sent us a new development contract of large sized KLTN crystal. This was a turning point. It was on the crystal that large corporations including IBM, Bell Labs, Toshiba, and NTT all failed for commercialization. Oxide succeeded in making this crystal into a product, driving NTT to offer investment in us, to secure the stable supply of the crystal. We were just a few people, and NTT was a company with hundreds of thousands of employees, so it was a surprise to us, but it also made us realize that small can control large in a situation that makes us imperative. A similar episode followed shortly. CLBO crystal, which was invented at Osaka University, was necessary material for UV laser devices, but big businesses had withdrawn from growing it. Responding to users' requests, we worked on it, improved the quality, and made its supply stable. This drove businesses within Japan and in the US to invest. From these, we learned that one of our missions as a venture business was to challenge what large corporates cannot tackle.

Recently, especially in Japan, many large businesses quit the crystal business one after another. In 2015, we took over the business of LGSO scintillator crystals from Hitachi Chemicals, recognizing their importance in society. Our revenue at the time was JPY1.4B, whereas the investment needed was JPY1B, so it was a difficult decision. After 3 years, we were able to raise the quality and yield to the best in the world, and the business had turned profitable. These are now deployed in state-of-art cancer detection PET instruments and saving many lives. In 2010, we took over the UV laser business from SONY. In 10 years the performance was dramatically improved, and we now have >90% of the global market share of nonlinear crystals for semiconductor inspection applications.

In 20 years after establishment, we grew to a group of experts, taking over technologies and personnel from large businesses. We now hold >300 patents, are >200 employees, and contribute to the local industry and job market. We went public in 2021. We came with the wish of "Help the society by the research fruition in crystal and light". We shall keep this spirit to further grow the business and to be a role model for manufacturing venture businesses for future entrepreneurs.

Optimization of crystal growth and material parameters through in-situ energy-resolved neutron imaging

A. S. Tremsin[1,], D. Perrodin[2], A. S. Losko[3], S. C. Vogel[3], A. M. Long[3], T. Shinohara[4], K. Oikawa[4], J. J. Derby[5], W. Kockelmann[6], G. A. Bizarri[2], E. D. Bourret[2]*

[1]University of California at Berkeley, Berkeley, CA 94720, USA
[2]Lawrence Berkeley National Laboratory, Berkeley, CA 94720, USA
[3]Los Alamos National Laboratory, Los Alamos, NM 87545, USA
[4]Japan Atomic Energy Agency, Naka-gun Ibaraki 319-1195, Japan
[5]University of Minnesota, Minneapolis, MN 55455, USA
[6]ISIS Facility, Rutherford Appleton Laboratory, Chilton, OX11 0QX, United Kingdom

Certain applications and technologies rely on the existence of single crystal materials. In many cases the discovery of new materials for these applications, typically performed on powder or small crystal samples, needs to be followed by the growth of large single crystals. Uniformity of the crystals is critical as light scattering and charge trapping occurring at defects substantially degrade the performance of detection devices. It is the development of crystal growth recipes, which in many cases, becomes the most difficult, long and expensive part of novel material transition from the discovery phase into large scale production for detection devices. The trial and error approach frequently used in the past is very costly and time consuming as growth can take days to weeks.

Inherently many crystal growth techniques do not allow direct measurements during the growth, such as in case of hygroscopic or highly reactive materials, which are usually grown in a vacuum-sealed container by the Bridgman-Stockbarger technique. Energy-resolved neutron imaging provides the means for in-situ diagnostics during crystal growth due to high penetration capability of neutrons. In this talk we describe the relatively new capabilities of energy-resolved neutron imaging to provide in-situ diagnostics of crystal growth processes. We present the results of experiments where neutron imaging enabled direct observation of the location and the shape of the interface between the solid and liquid phases (Fig. 1). We also demonstrate how the speed of crystal growth can be optimized through neutron imaging, which also provides information on the elemental distribution in both liquid and solid phases and can even quantify the diffusion of some elements within and between these two phases.

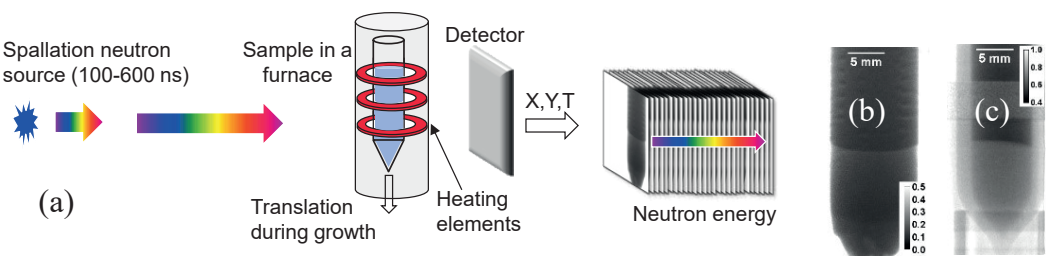

Figure 1. (a) Schematic diagram of energy resolved neutron imaging of crystal growth process in a Bridgman furnace. Neutron transmission spectra is measured in each pixel of the imaging data set, all energies simultaneously in one experiment. **(b),(c)** – concave and convex interface shape measured during crsytal growth of BaBrCl:Eu (b) and CsI:Eu (c).

Growth of large diameter yttrium aluminium garnet crystals by Czochralski method

Jan Polák, Jan Havlíček, Karel Bartoš, Jindřich Houžvička

Crytur spol. s r. o., Palackého 175, 51101 Turnov, Czech Republic

Presenting author:jan.havlicek@crytur.cz

Yttrium aluminium garnet (YAG) is a well-known oxide material for optical applications. YAG exhibits good mechanical properties, chemical and thermal stability and wide transparency range. It is a suitable host material for many dopant ions and it can be produced in a commercial scale. YAG single-crystals are mainly produced by Czochralski method (CZM). CZM production of YAG has been utilized for decades, however, there are still new challenges in this technology. One of them is the production of YAG crystals with a large diameter and high optical quality. This presentation introduces state-of-the-art undoped, Ce^{3+} doped and Yb^{3+} doped YAG crystals, manufactured by CZM in the Crytur company, with a diameter of 100-140 mm and weight up to 10 kg. Undoped YAG crystal is an excellent material for UV, VIS and IR optical elements, particularly for high energy density applications. Unlike sapphire, YAG is not birefringent, due to its cubic structure. Ce^{3+}:YAG is a scintillation material with good light yield and scintillation kinetics and can be applied in light conversion applications as well. Yb^{3+} doped YAG is a promising laser material with broad absorption bandwidth. It generates 1030 nm laser output pumped at 940 nm. Large diameter of Yb^{3+}:YAG crystal enables manufacturing of large slabs for high power-applications.

Challenges in the Growth of Large Size Scintillator Single Crystal

Shashwati Sen*, B Tiwari, M Tyagi, S G Singh, D G Desai, M Ghosh, S Pitale, G D Patra, A K Singh
Crystal technology Section, Technical Physics Division, Bhabha Atomic Research Centre, Mumbai, India
***shash@barc.gov.in**

The scintillators are those materials which generate spontaneous emission in the visible region when various kind of radiations viz X-ray, γ-ray photons, high energy charge particles and neutrons interacts with the material via the initial conversion of electrons and holes. These scintillator single crystals having broad transmission range along with superior mechanical and chemical stability and better radiation hardness are useful as radiation detector and used in the field of homeland security, high energy physics experiments, medical imaging among others. Though tremendous research has gone in this field, however till date growth of crack free and transparent big size crystal remains a challenge which can have application in the said area.

This talk will dwell on the challenges faced in the single crystal growth of the conventional scintillators like Tl doped CsI as well as the advance scintillators like Ce doped $Gd_3Ga_3Al_2O_{12}$, $YAlO_3$, LiI:Eu etc. The growth parameters of these single crystals were varied with an approach to improve the performance based on the systematic investigations. To increasing the diameter and length of the crystal the design of the growth station was also modified in few cases.

The growth of halide crystals like CsI:Tl and LiI:Eu crystals was carried out using the Bridgman method. Though this technique is relatively simple, however, disadvantages arise from the contact between container and melt/solid which can give spurious nucleation, sticking of the crystal ingot inside the crucible and consequently generating thermal and mechanical stresses. The quality of the source material and the quartz crucible was also found to play crucial role in getting transparent crystals having better energy resolution when applied as radiation detector. Therefore furnace design, thermal gradient, appropriate crucible material and shape was considered in designing a crystal growth system. One of the major problems during the growth of halide crystals are cracking of crystals during cooling that have been solved by making a slight but ingenious modification in the crystal growth system which will be presented. After addressing these issues Single crystals of CsI:Tl with 75 mm diameter and 100 mm length were successfully grown (Fig(a)).

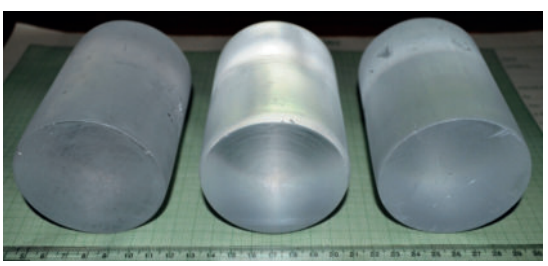

(a)

(a) CsI single crystal: 75 mm dia x 100 mm L (2 kg each)

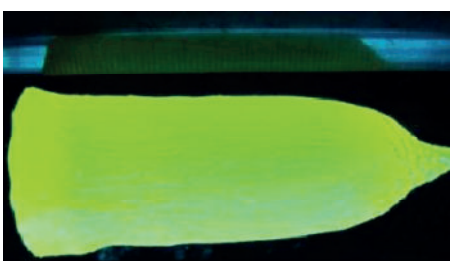

(b)

(b) $Ga_3Gd_3Al_2O_{12}$:Ce single crystal: 25 mm dia x 50 mm L

Advanced scintillator like Ce doped $Gd_3Ga_3Al_2O_{12}$ (GGAG:Ce) crystals having high melting temperature (~1900°C) with an optimized Ga to Al ratios of 3:2 was grown by Czochralski technique. The growth challenges faced were tackled by changing the stiochiometry, providing sufficient thermal gradient, carrying growth under suitable ambient, after growth annealing etc. Successful growth of one inch diameter and two inch length was achieved which was used to fabricated gamma spectrometer of energy resolution if ~7% at 662 keV.

IWCGT–8

Tuesday, May 31, 2022

LECTURES

Formation of secondary phase particles and the interplay mechanism with extended dislocations in CdZnTe bulk crystals

Yadong Xu[1,2]*

[1]*Key Laboratory of Radiation Detection Materials and Devices,*

[2]State Key Laboratory of Solidification Processing, *Northwestern Polytechnical University, Xi'an 710072, China*

* Email: xyd220@nwpu.edu.cn

The presence of SP particles significantly affects the optical and electronic properties of the bulk crystals as well as the surface perfection of epitaxial substrates. They appear not only in II-VI (e.g., CdTe, ZnSe), III-V (e.g., GaN), and IV-VI (e.g., SiC) compounds, but also in oxides and fluorides [1]. CdZnTe (CZT) crystals have been studied intensively due to their potential applications in X/γ-ray detection and the growth of HgCdTe epilayers. However, localized regions with SP particles (inclusions/precipitates) and induced dislocations are usually generated inevitably in as-grown or post-growth annealed CZT crystals [2-4], which are known to be detrimental to the charge collection for CZT detector, simultaneously to degrade the epilayers crystallization.

Here, we report the relationship between SP particles and induced dislocations in CZT bulk crystals. Two possible models for growth and multiplication of dislocation clusters are proposed on the basis of dissociation-diffusion and thermomigration-deformation, respectively. In addition, the formation of SP particles in the typical chalcogenide semiconductor and metal halide perovskite crystals is also revealed.

References:

[1] Peter Rudolph, Dislocation patterning and bunching in crystals and epitaxial layers-a review,Crystal Research and Technology, 2017,52: 1600171.

[2] Yadong Xu, Yihui He, Tao Wang, et al., Investigation of Te inclusion induced glides and the corresponding dislocations in CdZnTe crystal. Crystengcomm, 2012. 14(2): 417-420.

[3] Yihui He, Wanqi Jie, Yadong Xu, et al., Matrix-controlled morphology evolution of Te inclusions in CdZnTe single crystal. Scripta Materialia, 2012. 67(1): 5-8.

[4] Ningbo Jia, Rongrong Guo, Yaxu Gu, et al., Investigation of dislocation migration in substrate-grade CdZnTe, Journal of Crystal Growth, 2017, 457: 343-348.

Growth specifics of CdTe and related mixed systems

Peter Rudolph

Crystal Technology Consulting

rudolph@ctc-berlin.de

CdTe and (Cd,Zn)Te belong to the most important semiconductor materials with increasing application in various branches of life. Due to their relative high atomic numbers, high density and wide band-gap they show excellent spectral and spatial resolution for X- and γ-ray detection systems operating without cryogenics that benefits their application for medical imaging, industrial tomography, safety, and astrophysics. The same use is proposed for Cd(Te,Se) and (Cd,Mg)Te showing segregation coefficients of Se and Mg $k \approx 1$. Further, the tested efficiency of CdTe solar cells reached 22 %. Terahertz and photonic crystals are under current development too. (Hg,Cd)Te epitaxial layers on fitting (Cd,Zn)Te substrates represent the best composition for IR imaging devices already successfully used in thermal imaging cameras and strategic defense systems. Finally, a wide magneto-optical application is predicted for (Cd,Mn)Te and (Cd,Mn,Hg)Te.

Since the middle of last century there are strong efforts to master the bulk growth of high quality and productivity, especially of CdTe and (Cd,Zn)Te. However, from the beginning it became apparent that this proves to be a difficult undertaking. Why? Because of the extremely complex material properties differing the II-VI markedly from III-V compounds. Primarily these are: i) high ionic fraction of the binding force (> 60 %) responsible for high degree of association in the melt, enhanced dislocation mobility, and distinct dislocation patterning, ii) low stacking fault energy (10^{-6} J cm^{-2}) favoring twinning along the {111} faces, iii) low thermal conductivity in the crystalline phase (0.01 W cm^{-1}K^{-1}) being two times smaller than in the melt allowing only relative small growth rates and causing undesired concave growing interfaces, and iv) relative wide compound existence region deviated from stoichiometry toward Te excess ($x \approx 0.501$ at 1000°C) that promotes Te precipitation and probability of constitutional supercooling at the propagating interface. Thus, the long-standing question is how to master these drawbacks and which method proves to be optimum?

Mostly studied are *growth methods from melt* allowing the fastest crystallization velocity and, thus, the highest production rate. Besides horizontal and vertical Bridgman method, VGF and Czochralski techniques have been studied. However, independently on many tests of numerous ampoule types, additional Cd source for stoichiometry control, extra high total pressure, liquid encapsulation, ACRT or axial vibration etc. until today the production yield per ingot is lower than 50 %. The main reasons are i) high degree of melt association, retaining tetrahedral coordination, that affects the crystal orientation and growth kinetics, and ii) high growth temperature at which the stacking fault energy is the lowest and, thus, twinning probability the highest. The cardinal problem proves to be the too small overheating for breaking the melt structure even at seeded VGF. Against it, Czochralski growth would allow sufficiently high overheating before seeding but, curiously, the early reported very poor CdTe and (Cd,Mn)Te crystals, overcrowded with twins and grain boundaries, discouraged further attempts. But today the question arises for the author why the vapour pressure controlled Czochralski (VCz) with stoichiometry control and traveling magnetic field for melt stirring should not be a proper solution ?

Excellent 2-inch CdTe and (Cd,Zn)Te crystals of high structural perfection with RC FWHM of ~8 arcsec and low dislocation density $<10^4$ cm^{-2} can be grown by physical *vapour phase transport*. The atomically smooth interface allows the favourable step-by-step growth mode, e.g. when a seed with vicinal face is used. Further, the reduced growth temperature at ~800°C suppresses twinning. Additionally, the incorporation of Te inclusions should be minimized due to missing enrichment in a diffusion boundary layer. Nevertheless, this quite good method did not yet manage the transfer to the large-scale production due to its lowest growth rate. The maximum value so far of 2 mm d^{-1} was reported at VP THM.

Meanwhile, five of the worldwide leading seven manufacturers produce CdTe and (Cd,Zn)Te crystals by the travelling heater method (THM) from Te-rich *melt-solution* at about 800°C. Crystals with diameter of 75 mm and length up to 20 cm are obtained in rotating carbon-coated quartz tubes at growth rates around 5 mm d^{-1} and even higher. The decisional advantages are i) the relative low growth temperature suppressing twinning and reducing dislocation density, ii) the zone growth arrangement ensuring a homogeneous axial Zn distribution and in combination with optimized rotation a favourable slightly convex interface, and iii) the reduced segregation coefficients of impurities due to growth from solvent resulting in a higher crystal purity. Electrical resistivities of 10^{10} Ω cm and μτ products of 10^{-2} cm^2 V^{-1}, both important qualities for radiation detectors, were obtained by THM. However, problems still to be solved are the dislocation cell patterning affecting the carrier charge transport and the enhanced incorporation of Te microparticles from the solvent zone. To counter this an intensive steady zone stirring and a very harmonic slightly convex interface morphology without concavities and local grooves must be guaranteed. At the present ACRT modes are modelled and tested to remove the diffusion boundary layer most suitable. However, thereby appearing oscillating vortices still need to be mastered although at melt-solution growth the diffusion-driven interface relaxation behaves quite inertly.

Selected review literature:

- O. Limousin, Nuclear Instruments and Methods in Physics Research A 504 (2003) 24–37 (*X- and γ-ray detectors*)
- R. Triboulet, P. Siffert (eds.): CdTe and Related Compounds (Elsevier 2009) (*material properties, growth and application*)
- P. Rudolph, Progr. Crystal Growth and Charact. of Materials 29 (1994) 275- 380 (*melt growth fundamentals and measures*)
- A. Mycielski et al., Progr. Crystal Growth and Charact. of Materials 67 (2021) 100543 (*CdTe mixed with Mg, Se, Mn*)

TU | 02:10 pm

3D Metamaterials – Rationally Designed Artificial Crystals

Martin Wegener
Institute of Applied Physics, Institute of Nanotechnology, and Excellence Cluster *3D Matter Made to Order*,
Karlsruhe Institute of Technology (KIT), 76128 Karlsruhe, Germany
martin.wegener@kit.edu

Three-dimensional (3D) metamaterials are rationally designed 3D composites made of one or more bulk ingredient materials, allowing for effective-medium properties going beyond ("meta") those of their ingredients, qualitatively and/or quantitatively [1,2]. In this talk, I focus on 3D crystalline and 3D quasi-crystalline metamaterials.

After an introduction into the concept [2] and into the manufacturing by means of 3D laser nanoprinting [3], I discuss a variety of recent examples. I will not address 3D optical metamaterials, which we have been reviewed years ago [4]. Examples of 3D transport metamaterials include artificial cubic chainmail-like crystals leading to a sign reversal of the effective isotropic Hall coefficient [5,6], and anisotropic crystals exhibiting the parallel Hall effect [7].

Examples of 3D mechanical metamaterials include cubic crystals exhibiting a sign reversal of the isotropic thermal expansion coefficient [8] and a negative static isotropic volumetric effective compressibility [9,10], which appears to be forbidden energetically and thermodynamically at first sight. Furthermore, I will emphasize cubic and tetragonal chiral crystals [11-16], which can exhibit quasi-static twist effects as well as pronounced ultrasound acoustical activity [14-16] – the mechanical counterpart of optical activity. Finally, I will review our recent work on achieving roton-like acoustic-phonon dispersion relations by tailored beyond-nearest-neighbor interactions in 3D mechanical metamaterials [17,18].

I thank all coauthors listed below for their contributions. I acknowledge funding by the Deutsche Forschungsgemeinschaft (DFG, German Research Foundation) under Germany´s Excellence Strategy via the Excellence Cluster 3D Matter Made to Order (EXC-2082/1 – 390761711), by the Carl Zeiss Foundation through the "Carl-Zeiss-Focus@HEiKA", by the Helmholtz program "Science and Technology of Nanosystems" (STN) and the associated KIT project "Virtual Materials Design" (VIRTMAT), by the Karlsruhe School of Optics & Photonics (KSOP), and by the Max Planck School of Photonics (MPSP).

[1] M. Wegener, *Science* **342**, 939 (2013)
[2] M. Kadic, G.W. Milton, M. van Hecke, and M. Wegener, *Nature Rev. Phys.* **1**, 198 (2019)
[3] V. Hahn, F. Mayer, M. Thiel, and M. Wegener, *Opt. Photonics News* **30(10)**, 28 (2019)
[4] C.M. Soukoulis and M. Wegener, *Nature Photon.* **5**, 523 (2011)
[5] C. Kern, M. Kadic, and M. Wegener, *Phys. Rev. Lett.* **118**, 016601 (2017)
[6] C. Kern and M. Wegener, *Phys. Rev. Mater.* **3**, 015204 (2019)
[7] C. Kern, V. Schuster, M. Kadic, and M. Wegener, *Phys. Rev. Appl.* **7**, 044001 (2017)
[8] J. Qu, M. Kadic, A. Naber, and M. Wegener, *Sci. Rep.* **7**, 40643 (2017)
[9] J. Qu, A. Gerber, F. Mayer, M. Kadic, and M. Wegener, *Phys. Rev. X* **7**, 041060 (2017)
[10] J. Qu, M. Kadic, and M. Wegener, *Extreme Mech. Lett.* **22**, 165 (2018)
[11] T. Frenzel, M. Kadic, and M. Wegener, *Science* **358**, 1072 (2017)
[12] I. Fernandez-Corbaton, C. Rockstuhl, P. Ziemke, P. Gumbsch, A. Schroer, R. Schwaiger, T. Frenzel, M. Kadic, and M. Wegener, *Adv. Mater.* **31**, 1807742 (2019)
[13] V. Hahn, P. Kiefer, T. Frenzel, J. Qu, E. Blasco, C. Barner-Kowollik, and M. Wegener, *Adv. Funct. Mater.* **30**, 1907795 (2020)
[14] T. Frenzel, J. Köpfler, E. Jung, M. Kadic, and M. Wegener, *Nature Commun.* **10**, 3384 (2019)
[15] T. Frenzel, V. Hahn, P. Ziemke, J.L.G. Schneider, Y. Chen, P. Kiefer, P. Gumbsch, and M. Wegener, (Nature) *Commun. Mater.* **2**, 4 (2021)
[16] Y. Chen, Q. Zhang, T. Frenzel, M. Kadic, and M. Wegener, *Phys. Rev. Mater.* **5**, 025201 (2021)
[17] Y. Chen, M. Kadic, and M. Wegener, *Nature Commun.* **12**, 3278 (2021)
[18] J.A. Iglesias Martinez, M.F. Groß, Y. Chen, T. Frenzel, V. Laude, M. Kadic, and M. Wegener, *Science Adv.* **7**, eabm2189 (2021)

UV-C Transparent PVT AlN Substrates

Rafael Dalmau[1,a], Samuel Kirby[1,b], Jeffrey Britt[1,c], Raoul Schlesser[1,d]
[1]HexaTech, Inc., 991 Aviation Pkwy. Ste. 800, Morrisville, NC 27560 USA
[a]rdalmau@hexatechinc.com, [b]skirby@hexatechinc.com, [c]jbritt@hexatechinc.com, [d]rschlesser@hexatechinc.com

Ultrawide bandgap, low-dislocation-density aluminum nitride (AlN) substrates are highly sought for applications ranging from optoelectronics to high-power and high-frequency electronics. These substrates enable growth of AlGaN-based devices with low defect densities, leading to improved device performance. Recently, 2-inch diameter AlN substrates free of macrodefects and with average dislocation densities below 10^3 cm^{-2} have become commercially available [1, 2]. However, for optoelectronic devices requiring light extraction through the substrate, such as ultraviolet C (UV-C) light emitting diodes (LEDs), not only high substrate structural quality, but also low optical absorption coefficients at typical emitter wavelength of 265-280 nm are required for high device performance. AlN bulk crystals grown at high temperatures by physical vapor transport (PVT) commonly posses an absorption band around 265 nm, presenting a challenge for their use in UV-C emitters. Several groups have shown this absorption band is due to deep level midgap states originating from carbon impurities, which are commonly present in the PVT growth environment [3]. Beneficially, we demonstrated that co-doping with silicon is effective in suppressing the unwanted 265 nm absorption band, by forming a carbon-silicon defect complex, which shifts the absorption band deeper in the UV to 225 nm [4]. This approach resulted in commercially available 1-inch diameter substrates with absorption coefficients at 265 nm between 40 and 100 cm^{-1}. In this work, we subsequently grew and characterized large diameter PVT boules, Fig. 1, with varying concentrations of impurities, with a goal of further reducing the 265 nm absorption for 2-inch substrates. The boules were processed into ~400 µm thick, double-side polished substrates. Absorption coefficients were accurately calculated with an approximation-free method [5] from measurements of transmittance and absolute reflectance using a high-performance, double-beam, double-monochromator UV/Vis spectrophotometer [6]. As shown in Fig. 1, absorption coefficients at 265 nm as low as 12 cm^{-1} were achieved in 2-inch substrates. Furthermore, the complex refractive index and relative permittivity of AlN for the $\boldsymbol{E}\perp\boldsymbol{c}$ polarization at 295 K were calculated from the measured data, showing good agreement with published data for nominally unstrained bulk crystals. Reliable values for the high-frequency (optical) and static permittivities were also obtained. Finally, spatially-dependent absorption spectra, together with measured impurity concentrations from secondary ion mass spectrometry (SIMS) data, of large diameter, UV-C transparent AlN substrates will be presented, and the mechanism for reduction of UV-C absorption will be discussed.

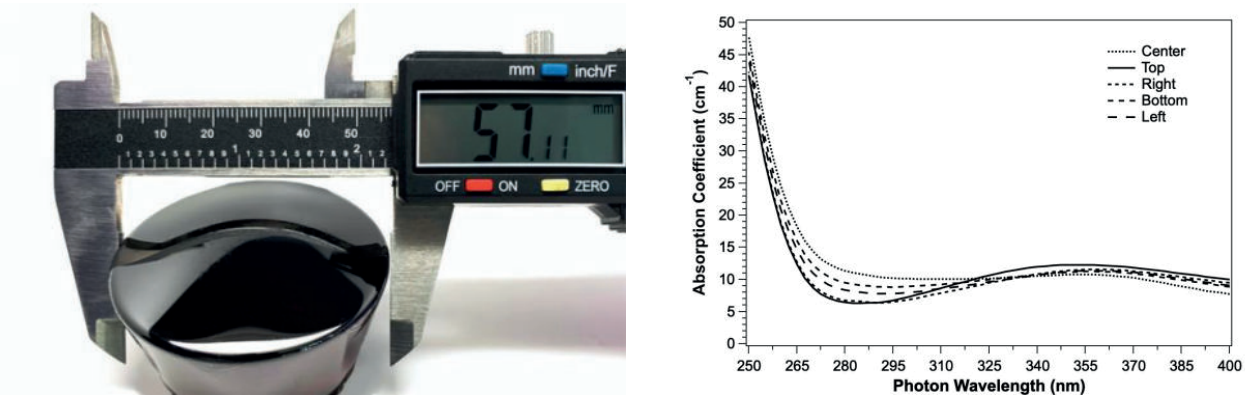

Figure 1. (*Left*) Image of a 57 mm diameter freestanding AlN boule grown by PVT. (*Right*) Reflection-corrected absorption coefficients of a 2-inch AlN substrate measured at five different points: center point; and top, right, bottom, and left points at a 40 mm diameter. A high spatial uniformity of optical properties and 265 nm absorption coefficients in the 12 to 18 cm^{-1} range are observed.

References:
[1] R. Dalmau *et al.*, Mater. Sci. Forum **924**, 923 (2018).
[2] R. Dalmau *et al.*, ECS Trans. **92**(7), 113-121 (2019).
[3] R. Collazo *et al.*, Appl. Phys. Lett. **100**, 191914 (2012); K. Irmscher *et al.*, J. Appl. Phys. **114**, 123505 (2013); I. Gamov *et al.*, J. Appl. Phys. **126**, 215102 (2019).
[4] B. Gaddy *et al.*, Appl. Phys. Lett. **104**, 202106 (2014)
[5] D. C. Look and J. H. Leach, J. Vac. Sci. Technol. B **34**(4), 04J105 (2016).
[6] R. Dalmau *et al.*, ECS Trans. **98**(6), 3-11 (2020); R. Dalmau *et al.*, ECS Trans. **104**(7), 49-56 (2021).

Evolution of Silicon Carbide Substrate Production/Understanding and Managing Defects in Silicon Carbide

P.S.Raghavan, onsemi, 5 Wentworth Drive, Hudson, New Hampshire, NH, USA
raghavan@onsemi.com

The growing demand for power electronic device for automotive, photovoltaic, transportation, motor drives creates an enormous demand for wide band gap semiconducting materials such as silicon carbide (SiC) and gallium nitride (GaN). While GaN based devices can be used for low voltages, SiC is the workhorse for voltages >600 volts. The adoption of wide-bandgap semiconductor devices made from materials like SiC will provide energy efficient devices that have almost no losses, creating a sustainable path to achieve net zero carbon emission. Shipments of SiC power devices, which are made on native single-crystal substrates, have climbed in recent years. This has enabled SiC to move out of the lab and establish itself as a mainstay for power electronic devices, especially when breakdown voltages greater than 900 V are required.

Progress in the availability of larger diameter SiC wafers has driven the final cost of device assembly down. Today, SiC is grown from a gas or liquid phase process that involves the following: (a) the generation of reactants (sublimation or non-congruent melt) (b) the transport of reactants to the growth surface (required temperature gradients), (c) adsorption at the growth surface (supersaturation), (d) nucleation and (e) finally crystal growth – advancement of gas solid interface or solid liquid interface.

In the case of SiC, the solid phase coexists in equilibrium with its gaseous phase and hence, it sublimes before it melts. As a result, since there is no stoichiometric SiC liquid phase, it is impossible to employ congruent melt growth and instead crystal growth from the vapor phase is the preferable technique for growing SiC crystals at a commercial scale.

While elemental semiconductor such as silicon can be grown as a totally defect free crystal, to the date SiC cannot be grown defect free due to the fundamental issues with vapor phase growth, multiple polytypes, spiral growth mechanism, low stacking fault energy, etc. While commercialization of 4H -SiC is aggressively pursued by leading suppliers of SiC substrates, structural defects such as micropipes, low angle grain boundaries, stacking faults, threading edge dislocations, basal plane dislocations and threading screw dislocations limit the device yield and performance.

The need for further improvements of quality and control of growth led to additional advances of the PVT process as well as the exploration of other viable options. The principle of gaseous cracking for the supply of Si and C was further developed in order to achieve growth rates comparable to the PVT method for the production of high volume wafers. The technique is called high temperature chemical vapor deposition (HT-CVD). Further concepts were presented such as the Halide CVD (H-CVD), Modified PVT (M-PVT) and a combination of HT-CVD and PVT reactor called Continuous Feed PVT (CF-PVT). However, the latter techniques are far from producing commercial scale SiC wafers and are currently used at an academic level.

In this talk we discuss the evolution of PVT SiC crystal growth process and maturity of the 150 mm and 200 mm diameter for mass production of SiC crystals and their characterization results, technology adoption and road to low cost SiC materials.

IWCGT–8

Wednesday, June 1, 2022

LECTURES

Can machine learning help us grow advanced crystals?

N. Dropka[a] and M. Holena[b,c]

[a] Leibniz Institut für Kristallzüchtung (IKZ), Max-Born-Str. 2, 12489 Berlin, Germany
[b] Leibniz Institute for Catalysis, Albert-Einstein-Str. 29A, 18069 Rostock, Germany
[c] Institute of Computer Science, Pod vodárenskou veží 2, 18207 Prague, Czech Republic
E-mail: natascha.dropka@ikz-berlin.de

The severe economic price pressure in the electronic and photovoltaic industries drives the development of the crystal growth technologies towards increased crystal grow yields of high quality crystals. Traditional experimental trail-and-error approach combined with global numerical modelling cannot provide optimized equipment design and process parameters in the real time. Particularly interdisciplinary nature of the crystal growth with its harsh process conditions, high crystal purity requirements, long process times, numerous constrained process parameters, unknown crystal material properties and the dynamic process character pose an increasing challenge.

One of the most exciting cutting-edge tools that entered the field of crystal growth over the last decade is machine learning (ML). It is a generic term for obtaining knowledge by a computer from experience, i.e. ML is a collection of statistical methods, both deterministic and stochastic, that has a great potential to revolutionize optimization of the crystal growth processes and equipment, process control and interpretability of the results in general.

Currently, ML applications are mushrooming in all fields of crystal growth and on all scales, from bulk to epitaxial growth, from numerical simulations to experiments and from atomic to macro scale.

Here we will provide an overview of the various applications of ML and closely connected data mining techniques in bulk crystal growth based on the available literature. In addition, examples of our own ML results will be shown and discussed. Focus will be put on reviewing the methods appropriate for a field with a small amount of data such as crystal growth, including: i) data generation aided by the Design of Experiments (DoE), ii) data interpretability using Decision Trees (DT), and iii) solving regression tasks with a support of Artificial Neural Networks (ANN) combined with active learning method.

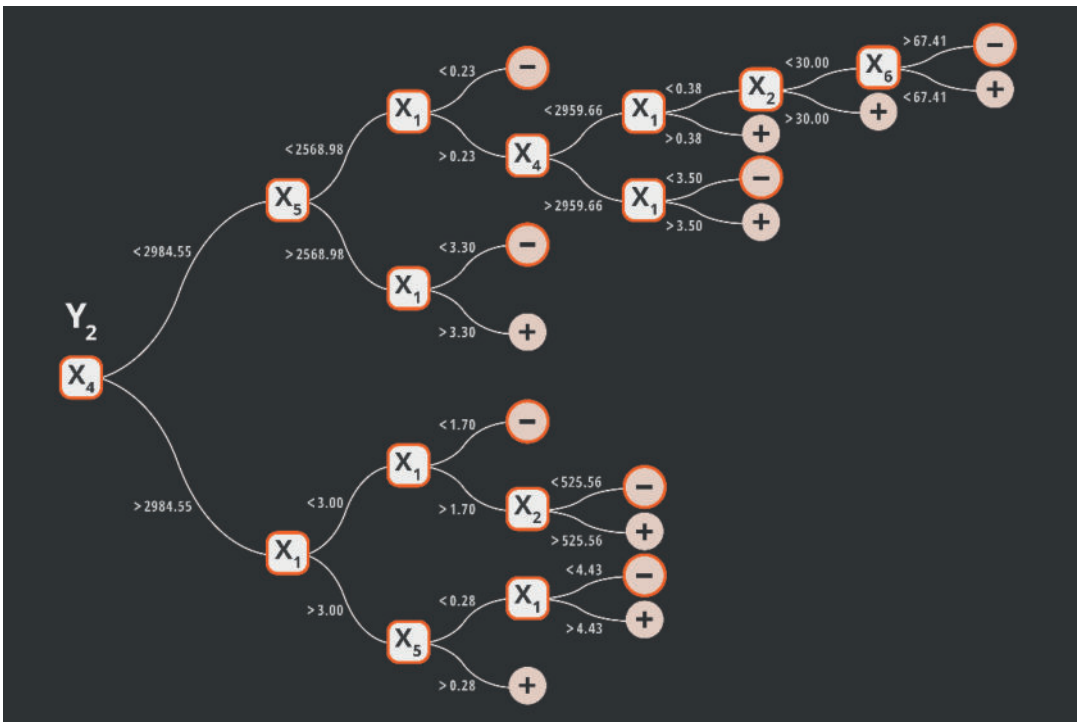

Fig. 1: Example of Classification Tree (kind of DT) machine learning techniques analyzing the dependence of the solid-liquid interface deflection y_2 on the power of heaters and growth rate x_1-x_6 in VGF-GaAs growth [1]. Courtesy of Anne Riemann (IKZ).

[1] Dropka, N., Böttcher, K., Holena, M., 2021. Development and optimization of VGF-GaAs crystal growth process using data mining and machine learning techniques. Crystals 11, 1218.

Big Data From Industrial Czochralski Silicon

Ludwig Stockmeier [1], Georg Raming [2]

[1] Siltronic AG, Berthelsdorfer Straße 113, 09599 Freiberg, Germany

[2] Siltronic AG, Johannes-Hess-Str. 24, 84489 Burghausen, Germany

ludwig.stockmeier@siltronic.com

Nowadays data is produced at increasing rate and size. The logic and storage of this data is mainly done on devices which base on semiconductors made from Silicon. This Silicon is grown by the Czochralski method, where the industry is highly digitalized. Not only the growth process by itself, which is automated as much as possible, but also everything which is linked to the growth process produces data. Digitalization of this industry has manifold reasons e.g. yield and product quality. In a customer quality-oriented industry, such as CZ industry, quality control is one of the main drivers to gather, store and work with data.

In this talk the data sources will be looked onto more closely. In CZ industry data is plentiful and the question of data usage / analytics / mining arises. Noticeably, the CZ process is a batch process and a substantial part of the data comes from outside of the CZ process, such as characterization results from wafers. Many parameters need to be considered, which affect the next growth run. Thus, not only one but many subject matter experts are involved when finding a solution or the root cause of an issue.

The 5V challenges for big data are data volume, variety, veracity, velocity and value. This 5Vs will be discussed in more detail in the context of CZ industry. Depending on the case different Vs can be considered as challenging. As an example, in one case the data volume is challenging since the amount coming from characterization tools can be too large and in another case the value is challenging, when a running system already exists e.g. diameter measurement.

A Short View On Optical Properties Of CZ Grown Germanium Crystals

Christian Hell[a]

a IV IR Optics GmbH, Am Goldberg 3, 99817 Eisenach
E-mail: christian.hell@iv-ir-optics.com

Summary

As a part of a research project, we have been working for improving the material parameters of germanium single crystals to get higher yields regarding critical parameters for optical mass fabrication. For standard purposes, most interesting parameters is optical homogeneity of the provided material. As homogeneity can be interpreted in different ways (resistivity, refraction and so on), the first thing to do was to find out what is most important. It pointed out that refractive index is the most necessary thing to know for this kind of applications. Due to many different values in literature, one of the main issues to solve, was to find out the correct values. Another task was to get high accuracy measurements and see if they are reliable enough to set them as a standard for future evaluations.
For determination of refractive index and homogeneity, a <111> orientated, n-type doped germanium crystal of 300mm diameter and 200mm length was grown. This crystal was cut completely to yield 165 samples to be measured for optical parameters.
Some of them were sent for counter measurements to NIST. The new established measurement system has been proven to be reliable regarding accuracy, repeatability and stability which was proved to better than expected. To get there, a huge amount of raw material was reserved and handled separately within the whole production and sample preparation process. As the interface between melt and crystal also varies by diameter, length, all experiments were performed on final industrial scale dimensions. A load of 12 crystals was grown in total, cut, and measured to see correlation between simulation, growth parameters and grown crystal. The results were the starting point for new calculations and modelling the crystal growth process itself.

Low Temperature Epitaxial Growth of Group IV Materials in View of Electrical Device Applications

Andriy Hikavyy[1], Roger Loo[1], Clement Porret[1], Gianluca Rengo[1,2], Erik Rosseel[1], and Robert Langer[1]

[1] Imec, Kapeldreef 75, B – 3001 Leuven (Belgium)
[2] Quantum Solid State Physics, KU Leuven, Celestijnenlaan 200D, B-3001 Leuven, Belgium
Corresponding author: Andriy.Hikavyy@imec.be

After five decades, CMOS scaling along Moore's Law is still alive and kicking, although its physical limits would have been reached already several years ago. At the beginning of the current century, the pure geometrical scaling came to an end and was followed by the so-called equivalent scaling, where the reduction of horizontal dimensions is combined with the introduction of new materials and new physical effects [1]. New vertical structures replaced the traditional planar transistor. In the next decades, scaling will continue, and we will enter the 3-Dimensional Power Scaling era, driven by reductions in power consumption [1,2]. Semiconductor industry predicts a transition to complete vertical device structures and monolithic integration which will be combined with heterogeneous device integration [1,2]. To a large extent, this ongoing success story is due to continuous materials innovations enabling complex device structures with nm-size dimensions. In this presentation we will focus on one important processing technique which is used to develop and fabricate new semiconductor materials, namely the epitaxial growth by means of Chemical Vapor Deposition. E.g. epitaxial growth enabled the implementation of alternative channel and source/drain (S/D) materials in logic devices which contributed to boost device performance [3,4]. The chosen alternative channel materials have a higher intrinsic electron or hole mobility as the Si equivalent. $Si_{1-x}Ge_x$ as S/D material is being used as stressor layer for the channels and to reduce contact resistance. Besides a control of the lattice constant and the electronic band gap, epitaxial growth also allows to reach high active doping concentrations without the need for high temperature post-epi annealing steps. The smaller electronic band gap and the high active doping concentration are used to reduce the contact resistance. More recently, epitaxially grown $Si/Si_{1-x}Ge_x$ and $Ge/Si_{1-y}Ge_y$ multilayers are implemented in the fabrication schemes of Si- and Ge-Gate All Around (GAA) devices, also known as nanosheet devices [5,6]. Depending on the need, any of these materials can serve as active or sacrificial layer. The sacrificial layer is selectively removed to reveal the nanosheets. Finally, there is a renewed interest in epitaxial strained $Si_{1-x}Ge_x$ as etch stop layer [7], which is being considered for 3-Dimensional System-On-Chip (3D-SoC) technology schemes. These schemes require wafer-to-wafer bonding combined with good control of the Si thickness and the Si within wafer uniformity [8].

Working with these modified device geometries and materials sets different requirements for the epitaxial growth steps in device fabrication. Accurate control over dimensions and thermal budgets are of prime importance to avoid variability and reliability issues. It is for instance imperative to avoid the relaxation and reflow of strained channels, significant materials intermixing and uncontrolled dopants diffusion. The situation becomes even more challenging when considering 3D stacked devices or chips as thermal budget constraints cumulate when front-end-of-line transistors and metal interconnects are already present (Fig. 2). Efforts are ongoing to reduce the thermal budget during epitaxial growth [9-11]. We will compare the growth characteristics of conventional precursors with those of higher order precursors and illustrate how the latter ones enables us to overcome the described challenges. Special attention will go to the epitaxial growth of S/D layers. The external resistance plays an important role in the device optimization. As a result, the active doping concentration in the S/D layers should significantly exceed the solubility limit.

References:

[1] P. Gargini, 2018 International Conference on Solid State Devices and Materials (SSDM), Special Short Course, p. 101
[2] R. Chau, 2019 IEEE International Electron Device Meeting (IEDM), p. 1.1.1
[3] R. Loo *et al.,* ECS Transactions 3 (7), 453 (2006)
[4] R. Loo *et al.,* ECS Journal of Solid State Science and Technology 6 (1), P14 (2017)
[5] H. Mertens *et al,* 2016 IEEE Symposium on VLSI Technology, p. 158
[6] A. Hikavyy *et al.,* Materials Science in Semiconductor Processing 70, 24 (2017)
[7] D. J. Godbey *et al*., Journal of the Electrochemical Society 137 (10), 3219 (1990)
[8] A. Jourdain *et a*l., 2018 IEEE 68th Electronic Components and Technology Conf. (ECTC), p. 1529
[9] C. Porret *et al.,* ECS Journal of Solid State Science and Technology 8 (8), P392 (2019)
[10] E. Rosseel *et al.,* ECS Transactions 93 (1), 11 (2019)
[11] A. Hikavyy *et al.,* Semiconductor Science and Technology 34 (7), 074003 (2019)
[12] A. Vandooren *et al,* 2018 IEEE Symposium on VLSI Technology, p. 69

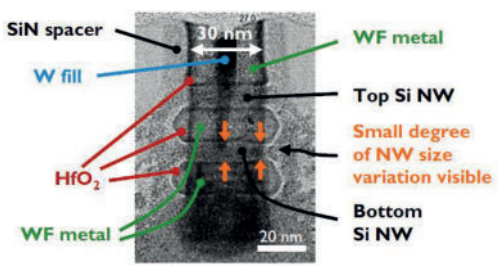

Fig. 1. Cross-section TEM of a Si channel GAA device [5].

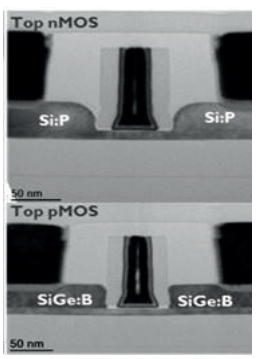

Fig. 2. Cross-section TEM of a 3D structure showing stacked devices [12].

Thursday, June 2, 2022

LECTURES

Recent Progress in Silicon Crystal Growth Technology for Solar Industry

Dr, Zhixin Li
CEO & CTO
Linton Crystal Technologies, Rochester, New York, USA
Linton Technologies Group, Dalian, China
lizx@lintonmachine.com

The solar industry is expected to grow more than a million tons of silicon mono-crystals this year for producing some 250 GW of solar modules. These modules can be used to generate enough electricity to meet the total power demand of either UK or Italy. Tens of thousands crystal growing furnaces operated by tens of thousands factory workers are mobilized to grow this large amount of crystals. In order to enhance productivity and reduce cost, many state-of-the-art technologies are used in crystal growth. These technologies include:

1. Large Czochralski furnaces with growing chamber ID of 1600mm or bigger;
2. Quartz crucibles larger than 36 inch in diameter, capable of containing more than 800 kg molten silicon and lasting more than 450 hours;
3. Fast growing techniques allowing growth rates of more than 100mm and 16kg per hour;
4. Recharge technology that allows up to 8 crystals being grown in series from the same crucible;
5. Advanced hot zone design reduces electricity consumption and increases productivity;
6. Precise diameter control reduces excessive silicon waste and reduces ingot machining time;
7. Automated furnace control software and HMI standardizes growth process, simplifies operation and operator training;
8. Central control system in the shop allows up to 100 crystal furnaces being monitored by a single person;
9. Advanced safety features provide fool-proof protection.

With the help of these technologies, the non-silicon growth cost of solar grade mono-crystals reduced more than 10 times during the past decade, greatly increased the competitiveness of solar power generation. The cost of photo-voltaic electricity is approaching 1 Euro cent per KWh, making it a strong candidate for replacing coal and hydrocarbon based power plants and a leader in green energy source.

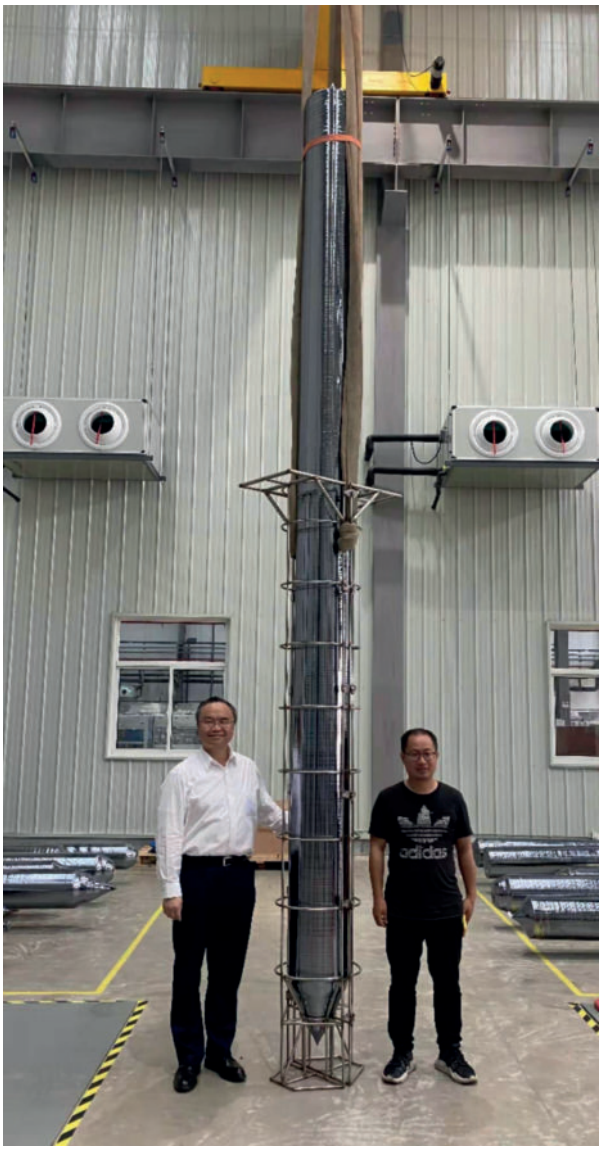

The above figure shows a Φ300mm silicon mono-crystal that is more than 5 meters long and weighs more than 800 kg, grown with a KX380PV furnace made by Linton Technologies Group.

Tools for the Industrial Production of Defect Controlled Silicon Ingots

Andreas Mühe[1], Alexey Denisov[1], Frank Mosel[1], Tse Wei Lu[2], Feng Hou Kun[2]
[1] PVA TePla AG, Im Westpark 10 – 12, 35435 Wettenberg, Germany
[2] Xuzhou Xinjing Semiconductor Technology Co., Ltd, No. 1 Xinxin Road, Xuzhou Economic and Technological Development Zone, Xuzhou, Jiangsu, China
Email corresponding author: andreas.muehe@pvatepla.com

The ongoing digitalization of all kinds of consumer goods as well as industrial investment goods is causing an ever-growing demand for high quality Silicon wafers. Especially, the supply of precisely point defect controlled 300 mm wafers for the mass production of latest design rule DRAM, NAND, CPU, and GPU is crucial. The physical mechnisms of point defect formation and agglomeration during the Czochralski-growth of Silicon crystals has been understood since more than 20 years, e.g. through the work of Voronkov [1] and others. Also, this understanding was extensively used in the numerical simulation of the point defect formation during the growing process [2, 3, 4] and applied to the design of hotzone and process recipes [5].

However, even today it is challenging for many players in the industry to mass-produce high quality defect controlled 300 mm Silicon ingots and wafers at a high yield and low cost. One of the reasons is the exceptionally high requirement for the precision and reproducibility in the control of the V/G distribution, both radially and axially throughout the ingots, as well as run-to-run and for each crystal growth furnace throughout the entire production facility.

In this presentation, we will discuss the various factors causing error margins to the spatial distribution of growth velocity and near-interface thermal gradient throughout the grown ingot, as well as run-to-run and furnace-to-furnace. Various technical solutions for the stabilization of the critical factors regarding the crystal growing furnace hardware, the hotzone, and the process control will be presented and some quality data of the achieved Silicon ingots will be shown.

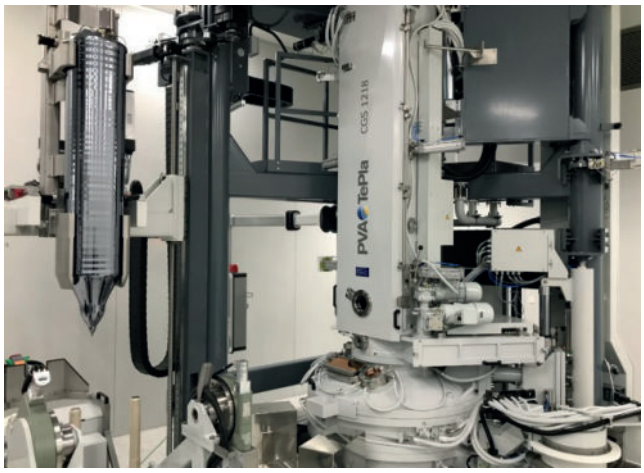

Fig. 1: 300 mm ingot grown from 280 kg charge size in the CGS 1218 puller

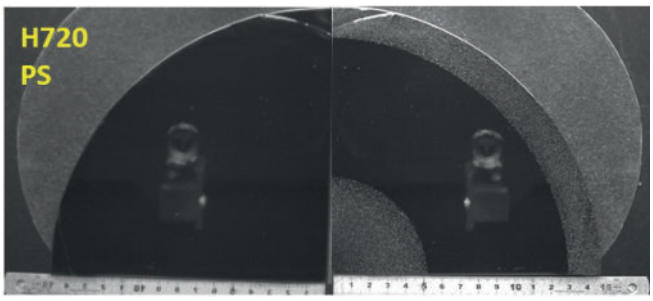

Fig. 2: Test slug characterization result after copper decoration. Left: No vacancy core or L-pit defect visible. Right: After enhanced thermal cycle, precipitate bands are delineated, however, no COP core or L-pit bands are visible.

References:

[1] V. V. Voronkov, R. Falster, "Vacancy and self-interstitial concentration incorporated into growing silicon crystals"; J. Applied Physics 86, (1999) 5975
[2] V.V. Kalaev, D.P. Lukanin, V.A. Zabelin, Yu.N. Makarov, J. Virbulis, E. Dornberger, W. von Ammon, "Calculation of bulk defects in CZ Si growth: impact of melt turbulent fluctuations"; J. Crystal Growth, 250/1-2 (2003) 203-208
[3] A. I. Prostomolotov, N. A. Verezub, "Two-Dimensional Model of the Intrinsic Point Defects Behaviour during Cz Silicon Crystals Growth"; Proceedings of SPIE - The International Society for Optical Engineering (2001)
[4] A. Muiznieks, I. Madzulis, K. Dadzis, K. Lacis, Th. Wetzel, "Simplified Monte Carlo simulations of point defects during industrial silicon crystal growth"; J. Crystal Growth 266 (1-3) (2004) 117-125
[5] Wen Ting Xu, Hai Ling Tu, Quing Chang, Quing Hua Xiao, Xiao Lin Dai, Yun Xia Liu, Zhong Feng Li, Lin Chang, Wei Da Liu, "Numerical Simulation of 300mm CZ Silicon Crystal Growth with Axial Magnetic Fields"; Materials Science Forum 689 (2011) 179-183

BAMAC – Kristallzüchtung

Wir stellen vor: Unseren hochauflösenden AtecFC-/AtexDC-Induktionsheizgenerator für Kristallwachstum auf Spitzenniveau

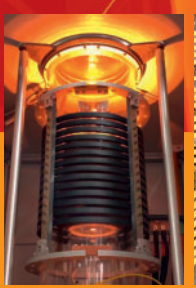

HOCHPRÄZISE
ZUVERLÄSSIG
DYNAMISCH
INDIVIDUELL

15 Jahre technischer Fortschritt garantieren eine maschinelle Fertigung auf höchstem Niveau – mit optimaler Zuverlässigkeit und absoluter Präzision.

- Reduzierte Betriebsgeräusche
- Vollständige Wasserkühlung, Luftkühlung oder Kombination beider Kühlungssysteme – je nach Kundenwunsch
- Flexibles Koaxialkabel oder wassergekühlte Hochstrom-Kupferschiene sowie andere Anschlusstypen möglich.
- Stabile und reaktionsschnelle Bedienung, die ideal an rapide Änderungen in der Netzversorgung und Belastung angepasst ist und die dynamische Stabilität verbessert.
- Benutzerdefiniert: Reverse Design je nach Induktionsspule. Arbeitsfrequenz, Gehäuse und Farbe können individuell angepasst werden.

Bamac Electric

No. 3800 HuQingPing Road
QingPu district · Shanghai
www.bamac.com

Vertrieb und Service in Europa

Max-Eyth-Straße 59
Deutschland
+49 208 41199797

Ihr Ansprechpartner für weitere Informationen:

Andreas Nebelung
andreas.nebelung@bamac-electric.de
+49 1517 4221708

POSTERS

Luminescence study of trivalent erbium ions doped into fluoride crystals grown by Bridgman method

Gabriel Buse[1], Marius Stef[1], Andrei Racu[1], Irina Nicoara[1], Daniel Vizman[1]
West University of Timisoara, 4 Bd.V. Parvan, Timisoara, 300223, Romania;
gabriel.buse@e-uvt.ro, marius.stef@e-uvt.ro, andrei.racu83@e-uvt.ro, nicoara1@yahoo.com, daniel.vizman@e-uvt.ro

Keywords: Fluoride crystals, Bridgman, Erbium Luminescence

Fluoride crystals (CaF_2, BaF_2, SrF_2 etc) have special physical properties, which give a variety of possibilities to use them in applications, both as passive optical media (optical windows, achromatic lenses, in the construction of prisms, infrared filters), but also as active optical media (laser active media, detectors or scintillators, etc.).

Er^{3+} ions doped in fluorite crystals have been studied especially for their emission properties generated by the higher conversion phenomenon [1,2]. Patel and co-workers showed that after excitation at 805 nm, the BaF_2: Er^{3+} crystal is efficient in generating red, green and UV radiation compared to the CaF_2: Er^{3+} crystal. Wojtowicz [3] studied VUV excitation and emission spectra and highlighted VIS, UV and VUV emission bands. The aim of this study is to compare the emission properties of the trivalent Erbium ion doped in the two fluorite matrices (CaF_2 and BaF_2) following excitation at around 376 nm to determine which host material is more efficient. The fluoride crystals in this study were grown by a resistive Bridgman graphite configuration. Also one of the purposes was to monitor the behavior of thermocouples in the graphite medium used in the Bridgman installation.

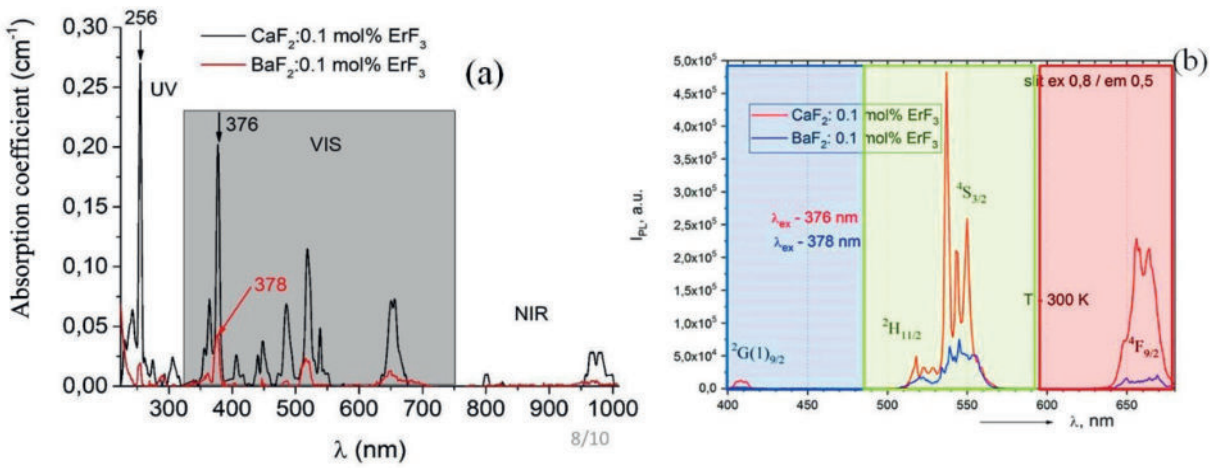

Fig.1. Comparison between (a) the absorption spectra, respectively (b) the emission spectra of the studied crystals

Absorption spectra at room temperature were recorded by the Shimadzu UV-1650PC spectrophotometer in the range of 190-1100 nm, and the emission spectra obtained by excitation in the absorption band around 376 nm were recorded using the FLS980-Edinburgh emission spectrophotometer (Figure 1). From the emission spectra it can be concluded that the CaF_2 matrix has higher spectroscopic properties than the BaF_2 matrix for excitation in the 376 nm band and have potential applications in the medical field (vascular hyperthermia-red band or photocoagulation – green band). Also, the use of a graphite based resistive configuration has an impact on the accuracy of the measured temperature values during the growths, being necessary a better protection of the thermocouples used for a much higher reproducibility of measurements.

References

[1] Patel, D.N., Reddy, R.B., Nash-Stevenson, S.K., Diode-pumped violet energy upconversion in BaF_2:Er^{3+}. Appl. Optic. 1998, 33, 7805–780.

[2] Bitam, A., Khiari, S., Diaf, M., Boubekri, H., Boulma, E., Bensalem, C., Guerbous, L., Jouart, J.P., Spectroscopic investigation of Er^{3+} doped BaF_2 single crystal. Opt. Mater. 2018, 82, 104–109.

[3] Wojtowicz, A.J., VUV spectroscopy of BaF_2:Er. 2009, Opt. Mater. 31, 474–478.

Poster 01

Self-learning crystal growth furnaces: perspective for artificial intelligence technologies

K. Dadzis, A. Enders-Seidlitz, I. Tsiapkinis

Leibniz-Institut für Kristallzüchtung (IKZ), Max-Born-Str. 2, 12489 Berlin
E-mail: kaspars.dadzis@ikz-berlin.de

Crystal growth processes are highly complex processes involving thermodynamics, heat transfer, fluid dynamics and many other phenomena taking place on a large range of spatial and temporal scales. The practical work of a crystal grower has been compared to that of an artist or even an alchemist [1]. However, the high relevance of crystal growth processes in various branches of modern industrial development requires a different point of view. Simultaneous handling of many input and output parameters needs sophisticated control algorithms and models, where the use of artificial intelligence (AI) and machine learning (ML) technologies may provide significant advantages. These have been already applied for crystal growth processes, however, mostly in the sense of supervised learning, where large experimental or numerical datasets are applied to *train* a predictive model (e.g., a neural network) [2]. A different approach is reinforcement learning (RL), which has shown extraordinary performance in games such as Chess and Go but is also of great potential for process control [3]. In this case, the AI engine is just given the "rules" and then is "learning" by itself, e.g., by playing Go game rounds against itself–or–by automatically growing crystals.

In this contribution, we examine the applicability of RL concepts to a crystal growth furnace on a hardware level for the first time known to the authors compared to earlier simulation studies (e.g. [4]). We use a fully automated but still very simple setup for the Czochralski growth of tin (melting point of 232 °C) in an air atmosphere. Compared to standard crystal growth equipment, this setup has the advantage of extensive in-situ measurement capabilities, flexible control interface as well as low safety requirements. In the first step, we consider the practically relevant goal of achieving a constant crystal diameter described by a linear increase of crystal weight. Melt temperature and crystal pull rate are used as control parameters. The figure below illustrates two automatic growth experiments with a fixed growth recipe. Crystal shape demonstrates good reproducibility. Next, we will apply Q-learning as a model-free RL algorithm [3] trained to produce crystals with a constant diameter. The reward function, which is maximized by the algorithm as a control goal, is designed to punish deviations from a prescribed linear weight increase. Both Q-tables and deep neural networks are investigated to approximate the Q-function. The algorithms are implemented in Python using the ML platform TensorFlow and integrated into setup automation running on a Raspberry Pi 4 microcomputer. To overcome the issue of high numbers of training cycles, the algorithm is first pre-trained in a simulation environment. While the control of crystal diameter using heating power and pull rate is a relatively simple goal often solved by PID algorithms, the potential of AI technologies is much higher. We discuss the possibilities to integrate into the RL algorithm additional parameters such as in-situ measured melt flow patterns or additional constraints such as maximum pull rate at minimal heating energy consumption.

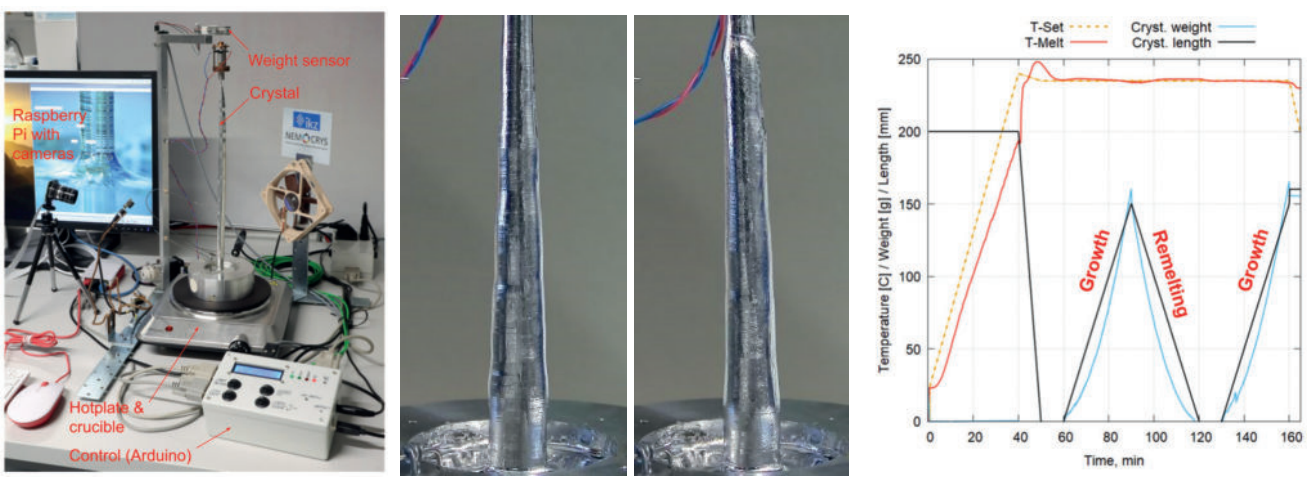

From left to right: Experimental setup for Czochralski growth; two automatically grown Sn crystals (remelting in between) with a prescribed growth recipe; time-dependence of melt temperature, crystal length and weight.

Acknowledgement: This work has been performed within the NEMOCRYS project funded by the European Research Council (ERC) under the European Union's Horizon 2020 research and innovation programme (grant agreement No 851768).

References:

1. J. Donecker, Phys. Bl. 52 (1996) Nr. 3, 248-249.
2. N. Dropka, M. Holena, Crystals 10(8), 2020, 663.
3. R. Nian, J. Liu, B. Huang, Comput. Chem. Eng 139 (2020) 106886.
4. L. Wang et al., Crystals 10(9), 2020, 791.

Analysis Of Bubble Engulfment During Melt Crystal Growth

Swanand Pawar and Jeffrey J. Derby*

Department of Chemical Engineering and Materials Science,
University of Minnesota, Minneapolis, MN, USA
*derby@umn.edu

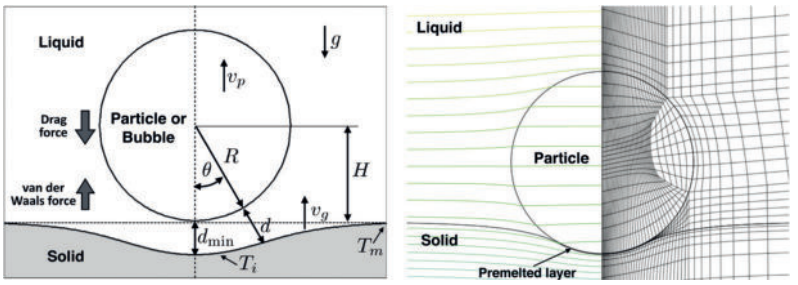

Figure 1: (a) A schematic depiction of particle/bubble engulfment during melt crystal growth. (b) Simulation of a solid particle being engulfed during growth, with temperature isotherms on the left and finite element mesh on the right.

Bubbles of 10–100 microns in size are often observed in sapphire and silicon crystals grown from the melt. Bubbles are defects, ruining structural uniformity, reducing the yield of high-quality material, and increasing costs. A better understanding of the fundamentals of bubble engulfment will provide a basis for improved material quality, increased process yields, and reduced costs.

The engulfment of bubbles during solidification is determined by a balance of repulsive van der Waals forces between the bubble and the solidification interface and drag forces arising from the flow around the bubble and into a thin liquid gap between particle and the solidification interface, typically on the order of 10 nanometers in thickness. When drag forces overcome repulsive forces, the bubble is engulfed, otherwise it is steadily pushed ahead of the advancing interface. There often exists a critical velocity at which a bubble of a certain size is engulfed, since drag generally increases with bubble size and velocity. However, drag forces are complicated by Marangoni flows along the bubble surface and upon the shape of the solid-liquid interface as the bubble approaches. Thus, the critical velocity is affected by significant and nonlinear interactions involving fluid dynamics, heat transfer, premelting, and Gibbs-Thomson phenomena.

We present efforts to develop, validate, and apply computational models to elucidate the mechanisms of bubble engulfment during melt crystal growth. This research builds upon prior steady-state and dynamic models at the continuum level that have been developed to study the pushing or engulfment of a solid particle at a moving, solid-liquid interface. Prior results have revealed new mechanisms that impact the engulfment of silicon carbide particles engulfed during the growth of multi-crystalline silicon [1]–[5]. Preliminary results will be presented for the engulfment of a gas bubbles during sapphire and silicon crystal growth.

[1] Y. Tao, A. Yeckel, and J.J. Derby, "Steady-State and Dynamic Models for Particle Engulfment during Solidification," *J. Comp. Phys.* **315,** 238–263 (2016).

[2] Y. Tao, A. Yeckel, and J.J. Derby, "Analysis of particle engulfment during the growth of crystalline silicon," *J. Crystal Growth* **452,** 1–5 (2016).

[3] J.J. Derby, Y. Tao, C. Reimann, J. Friedrich, T. Jauss, T. Sorgenfrei, and A. Cröll, "A quantitative model with new scaling for silicon carbide particle engulfment during silicon crystal growth," *J. Crystal Growth* **463,** 100–109 (2017).

[4] J.J. Derby, "The synergy of modeling and novel experiments for melt crystal growth research," IOP Conf. Ser.: Mater. Sci. Eng. **355** (2018) 012001.

[5] Y. Tao and J.J. Derby, "The engulfment of a precipitated particle in a saturated melt during solidification," *J. Crystal Growth* **577,** 126400 (2022).

This work was supported in part by the U.S. National Science Foundation, under CMMI-1853512. No official endorsement should be inferred.

Analysis Of Single-Crystal Diamond Growth Via HPHT

Scott S. Dossa[1], Ilya Ponomarev[2], Boris Feigelson[3], Marc Hainke[4,5], Christian Kranert[5], Jochen Friedrich[5], and Jeffrey J. Derby[1,*]

[1]University of Minnesota, Minneapolis, MN, USA; [2]Euclid Beamlabs, LLC, Beltsville, MD, USA; [3]U.S. Naval Research Laboratory, Washington, DC, USA; [4]Ostbayerische Technische Hochschule, Amberg-Weiden, Germany; [5]Fraunhofer IISB, Erlangen, Germany

*derby@umn.edu

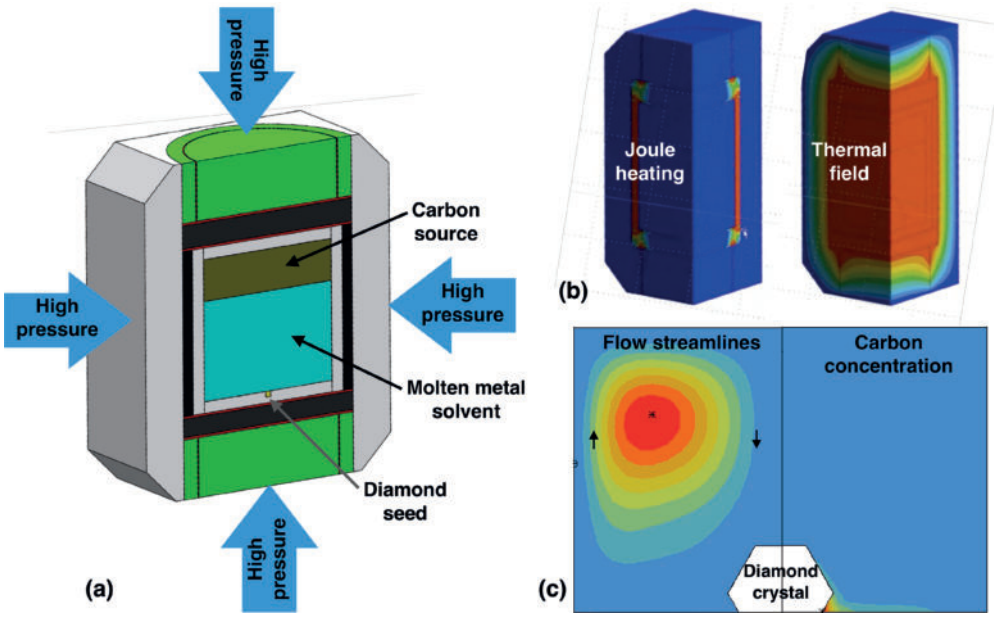

Figure 1: (a) A diamond single crystal, several millimeters in size, is grown from a metal solvent under extreme pressures and temperatures in a High-Pressure, High-Temperature (HPHT) cell. (b) 3D models of Joule heating predict system temperatures, and (c) finite-element models compute solvent flows and carbon concentration during growth.

Poster 04

The increasing power of X-ray optical sources and more stringent requirements of optical devices demand purer and more ideal materials. Large, single-crystal diamond is one of the few materials, if not the only, suitable for high power X-ray optical applications due to its unique combination of high thermal conductivity, low thermal expansion, and low X-ray absorptivity. Diamond single crystals are also of great interest for quantum computing and other industrial and medical applications.

The High-Pressure, High-Temperature (HPHT) crystal growth system has the capability to grow diamonds of the highest crystalline quality, with dislocation densities lower than 10 cm^{-2}. However, this near-equilibrium process is carried out under extreme conditions, where diamond single crystals are grown from a molten metal solvent (Fe, Ni, and Co and their alloys) under pressures in excess of 5 GPa (50,000 atmospheres) and temperatures of 1,600 K and higher. Since there are no available diagnostics to directly monitor crystal growth in the HPHT cell, faithful models are needed to connect experimental outcomes to system design and process conditions.

We present initial results from a collaboration that includes experimental growth carried out at the U.S. Naval Research Laboratory (Fig. 1a) and two modeling efforts. Detailed, 3D models are applied to describe electromagnetic heating the HPHT furnace by the Fraunhofer IISB (Fig. 1b). Temperature profiles from these analyses are employed in finite-element models by the University of Minnesota to predict flows and carbon transport through the growth cell (Fig. 1c). These models provide rigorous tools to both understand growth in this system and to perform subsequent optimization. In particular, we aim to more fully understand fundamental aspects of diamond nucleation and growth and identify process conditions that will achieve the highest crystalline quality in large diamond crystals.

This work was supported in part by the U.S. Department of Energy, under DE-SC0020604. No official endorsement should be inferred.

Solidification of the large diameter uniform Sb doped germanium crystals

Florin Baltaretu[1] and Michael Gonik[2]

[1]*Technical University of Civil Engineering, Bucharest, Romania,*
e-mail: florin.baltaretu@instal.utcb.ro
[2]*Centre for Material Researches 'PHOTON', Alexandrov, Russia,*
e-mail: michael.a.gonik@gmail.com

Germanium is widely used in modern IR-band optical system to produce windows and lenses. Czochralski standard technique is the most popular one for these purposes. However, in case of large diameters from 200 and up to 420 mm, modified Cz technique allowing to grow thin monocrystalline disks by directional solidification [1] or a horizontal directed crystallization resulting in polycrystalline germanium [2] are being more effectively to apply. In general, the range of free electron concentrations should lie approximately between $4 \cdot 10^{14}$ and $5 \cdot 10^{13}$ cm $^{-3}$ but better optical properties could be achieve in a more narrow range. To provide such homogeneity across a germanium disk is a rather complicated problem. And in addition, one has to maintain the necessary dopant concentration all over the height of the ingot.

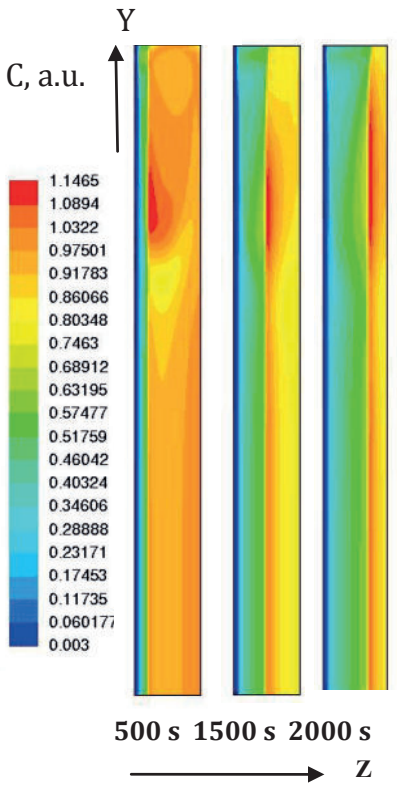

Fig. 1. Sb distribution in solidifying Ge layer: *D*=200 mm, *h*=10 mm.

Recently [3] we have discussed an opportunity to solidify a thin melt layer of Sb doped Ge by use of the axial heating process. Once the initial melt layer of a diameter *D* and with a thickness *h* is well stirred, for example, by electro-magnetic field [4], the heating from above results in uniform lateral dopant distribution during crystal growth owing to diffusion character of the mass transfer. The only small portion of the layer in the periphery depending on *h/D* ration was found to be inhomogeneous (see Fig. 1) due to the melt flow presence (vortex) caused by heat exchange at the side boundary.

In this work, first of all, we investigate the problem of heat and mass transfer with most realistic boundary conditions, which could give a more accurate analysis of *h/D* range influencing the limits of the diffusion approach application. For this purpose, we apply the finite volume method and SIMPLE algorithm to solve the partial derivative equations describing the physical phenomena of crystal growth, in the framework of the ANSYS Fluent package.

Under these conditions the axial dopant distribution strongly depends on temperature variation on the both hot (upper) and cold (bottom) [3] shown to be non-linear one in order to provide necessary Sb concentration and to complete the process for reasonable period. Previously we used the Tiller's relation to find the appropriate crystal growth rate as function of the z coordinate. And only at the next stage, it was possible to find the hot and cold temperature distribution itself. Now we have stated the inverse problem and offer to use an optimization module in an outside loop from the CFD software (and run the CFD simulation repeatedly). However, this could lead to some problems regarding the coupling of two different software and to quite a long time of simulation. The mathematical theory on this kind of problems involves the use of a functional that should be minimized - in this respect seems to be very close to a finite element procedure. Therefore, the possibility of using an integrated approach (CFD + optimization) in the same software was studied to realize the algorithm by COMSOL, which uses the finite element method and has the necessary optimization module.

Preliminary results on temperature regime of solidification resulting in a proper axial segregation and the dopant distribution in the crystal are presented.

[1] I.A. Kaplunov, E.I, Kaplunov and A.I. Kolesnikov. J. of Siberian Federal University. Engineering & Tech., 2013, 6(3) 324-333.
[2] G.S. Pekar, A.F., Singaevsky , M.M. Lokshin , V.I. Gordienko , I.V. Mazurin. Semiconductor Physics, Quantum Electronics & Optoelectronics, 2018. V. 21, N 2. P. 173-179.
[3] M.A. Gonik, F. J. Baltaretu. Cryst. Growth. 2019. V. 525 (1). 125166.
[4] X. Wang, D. Bliss, G. W. Iseler and N. Ma. J. of Thermophysics and Heat Transfer 19(1):95-100, 2005.

Crystal growth of the large-scale semiconductor crystals by the modified Cz method

Florin Baltaretu[1] and Michael Gonik[2]

[1]*Technical University of Civil Engineering, Bucharest, Romania,*
e-mail: florin.baltaretu@instal.utcb.ro
[2]*Centre for Material Researches 'PHOTON', Alexandrov, Russia,*
e-mail: michael.a.gonik@gmail.com

Germanium and silicon are still the more used materials in electronics and other applications. And as previously the main trend is to increase a diameter of the ingot. Taking into account the limits of the FZ technique (for example, for Si the theoretical maximum dimension is around 250-300 mm), Cz method seems to be the leading one to obtain large single crystals. However, the cost of the production increases with each inch because production needs more else bigger crucibles, application of the more power and complicated magnetic field and so on. Meanwhile these difficulties can be overcome by using during solidification the submerged in the melt the heating element (see Fig. 1), for example, an electrically conducting foil in case of oxides crystal growth [1]. Such an approach makes it possible (i) to grow crystals with a diameter very close of that of the crucible and (ii) better thermal control for the process of the solidification. The last is very important in producing of low dislocation density Ge being applied as a substrate for PV element in space industry. Use instead of a simple heating plate the AHP heater equipped with thermocouples (see Fig. 2a) open the way to provide the small axial temperature gradient close to the crystallization front all over the cross-section of the growing crystal.

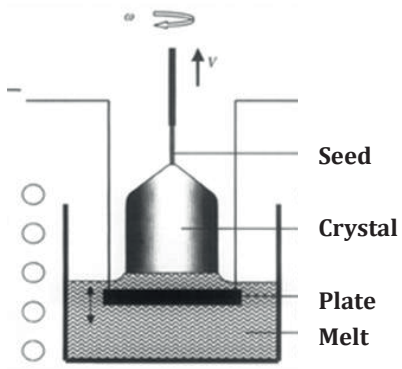

Fig. 1. Modified Cz technique

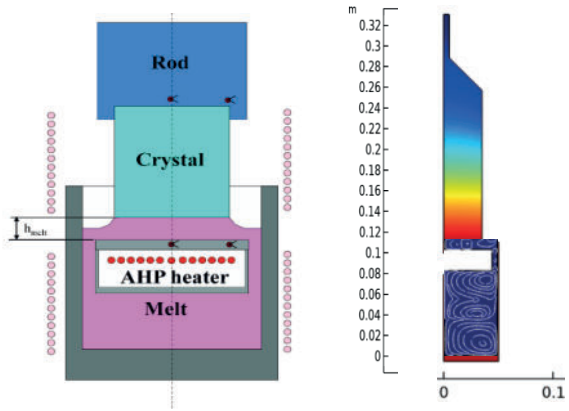

a) b)

Fig. 2. Schematics (a) of the AHP realization and calculation domain (b) together with results of computations

The main attention is paid to studying the influence of the submersed heater on melt convection, especially, close to the growing crystal, as well as possibility to govern the temperature field in it by varying the surrounding temperature. For these purposes we consider the calculation domain shown in Fig. 2b which allow to mathematically describe the process of solidification at all the stages of the crystal growth of 70 mm in diameter and 200 mm high. We vary in time the side boundary temperature (in fact, along the crucible wall and shields) in such a manner to provide the heat exchange of the top side surface of the crystal high enough to remove the latent heat from the front of crystallization. From the other hand, the temperature of the wall, at least, over the one diameter distance from the interface is maintained almost equaling to that of the crystal side to completely prevent the heat exchange and make here only the axial character of the heat flux resulting in one-dimensional temperature field and, consequently, in low density dislocations pattern. To analyze the character of the convection for dimension of the crystal of 500 mm in a diameter typical for Si solidification, we limited ourselves, at this stage of computations, by the melt zone only between submerged heater and the growing crystal.

Stability of the meniscus and its shape development during the solidification is under consideration from the point of view of the control of the process, first of all, the constant diameter of the crystal.

[1] B.S. Red'kin, V.N. Kurlov, I.S. Pet'kov, S.N. Rossolenko, J. Crystal Growth, v. 104, 1990, p. 77

Revisiting the growth of large (Mg,Zr):$SrGa_{12}O_{19}$ bulk crystals: Core formation and its impact on structural homogeneity revealed by correlative X-ray imaging

C. Guguschev [a], C. Richter [a], M. Brützam [a], K. Dadzis [a], C. Hirschle [b], T.M. Gesing [c,d], M. Schulze, A. Kwasniewski [a], J. Schreuer [b], D. G. Schlom [e,f,a]

[a] Leibniz-Institut für Kristallzüchtung, Max-Born-Str. 2, 12489 Berlin, Germany
[b] Institut für Geologie, Mineralogie und Geophysik, Ruhr-Universität Bochum, Universitätsstraße 150, 44801 Bochum, Germany
[c] University of Bremen, Solid State Chemical Crystallography, Institute of Inorganic Chemistry and Crystallography/FB02, Leobener Str. 7, Germany
[d] MAPEX Center for Materials and Processes, Bibliothekstraße 1, D-28359 Bremen, Germany
[e] Department of Materials Science and Engineering, Cornell University, Ithaca, NY 14853-1501, USA
[f] Kavli Institute at Cornell for Nanoscale Science, Ithaca, NY 14853, USA

E-mail: christo.guguschev@ikz-berlin.de

We demonstrate the growth of large (Mg,Zr):$SrGa_{12}O_{19}$ (SGMZ) single crystals and apply a combination of X-ray imaging techniques to analyze them structurally and chemically. Single crystal cylinders with lengths above 1 inch and diameters up to about 1 inch (Fig. 1a) were achieved by top-seeded solution growth with optimized melt compositions as explored by the pioneering work of Mateika and Laurien [1]. In the central parts of the grown crystals, we observed a similar stress-induced birefringence as published forty years ago. As a possible explanation, we considered the formation of a small (0001) facet at the central part of the growth interface which should have a detectable impact on both the chemical composition and the crystal lattice. In order to test this assumption, we developed a rocking curve imaging technique (Fig. 1b) with high sensitivity to study subtle variations of the microstructure [2].
This novel method enabled us to observe that the core region exhibits a reduced unit cell volume and is surrounded by a ring with increased lattice tilt and elastic strain. These effects were also analyzed using numerical simulations of the three-dimensional elastic stress and strain fields. Furthermore, variations of the cell volume in the outer parts of the crystal reveal a slight in-plane anisotropy of dopant incorporation following the hexagonal crystallographic symmetry. The relationship between unit cell dimensions and composition was verified by micro X-ray fluorescence mappings. With rocking curve widths below 23 arcsec in ~90 % of the crystal, the SGMZ crystals are largely homogeneous and hence well suited for the preparation of high-quality substrates. For most applications (e.g. as substrate for epitaxy of multiferroic $BaFe_{12}O_{19}$ thin films), the enhanced crystal size enabled by co-doping with Mg and Zr outweighs the issues related to concentration variations arising from their addition.

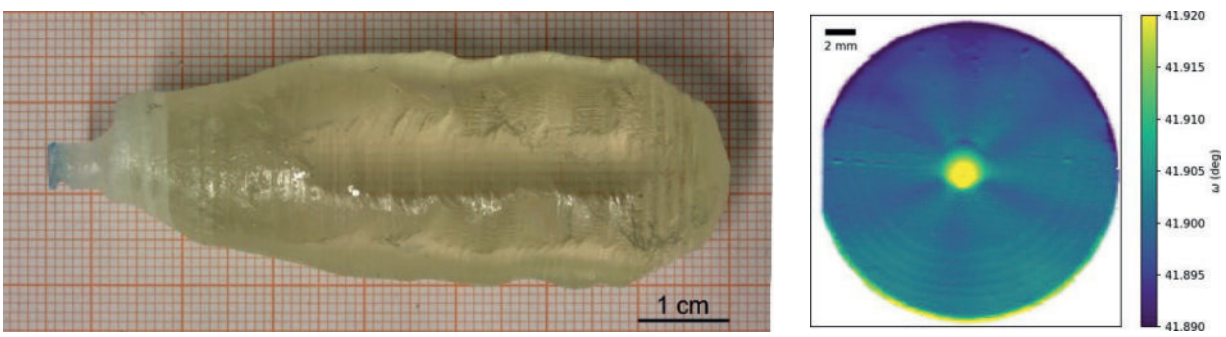

a b

Fig. 1: (a) Most recent SGMZ single crystal grown by the top-seeded solution growth technique (TSSG). (b) 2D distribution of the 0 0 0 20 peak position measured for a polished (0001) substrate of a SGMZ crystal as a first demonstration of the novel rocking curve imaging technique.

[1] D. Mateika, R. Laurien, Czochralski growth of solid solutions of strontium hexagallate with magnesium and zirconium as dopants, Journal of Crystal Growth, 52 (1981) 566-572.
[2] C. Guguschev, C. Richter, M. Brützam, K. Dadzis, C. Hirschle, T.M. Gesing, M. Schulze, A. Kwasniewski, J. Schreuer, D.G. Schlom, Revisiting the growth of large (Mg,Zr):$SrGa_{12}O_{19}$ single crystals: Core formation and its impact on structural homogeneity revealed by correlative X-ray imaging, Crystal Growth & Design, in press, DOI: 10.1021/acs.cgd.2c00030, (2022).

Growth of high quality CdZnTe bulk crystals using the Vertical Gradient Freeze technique

Timotée Journot[1], Erik Gout[1], Marc Parent[1], David Collonge[1], Samira Grief[1], Nicolas Lopez[1], Philippe Ballet[1]

(1) Université Grenoble Alpes, CEA-LETI, 17 Avenue des Martyrs, F-38054 Grenoble, France
Contact : timotee.journot@cea.fr

CdTe and CdZnTe are compound of choice to make both radiation detectors and high yield infrared Focal Plane Arrays (FPAs). These applications require single crystalline materials of high perfection because every material defect contributes to the degradation of the final detectors. For many years, the growth of CdTe and CdZnTe bulk crystals has been studied at CEA-LETI to make substrates for the epitaxy of HgCdTe that will be used as the active layers of infrared sensors[1]. The Zn addition is a versatile tool to tune the lattice parameter of the crystal and, thus, to make lattice matched substrates for the growth of HgCdTe compound at a given composition. Today, the crystals defects observed in the CdZnTe substrates, particularly the dislocations, are identified as sources of degradation of the final FPAs[2]. Thus, to continue improving the yields of the infrared sensors based on II-VI materials, we are working on dislocation density reduction in CdZnTe compounds.

Dislocations are one-dimensional crystal defects. Then, by nature, it is difficult to visualize and characterize them. Their density in CdZnTe substrates is commonly estimated using the Etch Pit Density (EPD), a chemical revelation of dislocations that cross the surface of interest. Today, the reported EPD measured in CdZnTe substrates are in the range 1-5.10^4 cm^{-2} [2–4].

The origins of these defects are multiple and complex. Among them, we find the relaxation of thermomechanical stress, the collapsing of point defects that are numerous because of the non-stoichiometry of CdTe alloys, the presence of the second phase defects. In this paper, we demonstrate that dislocation density reduction is achievable to reach EPD as low as 2.10^3 cm^{-2} in CdZnTe. Major progress has been achieved with dedicated multi-zones furnace to control the thermal gradients and the Cd partial pressure all along the crystal growth process. Both physical parameters enable us to get this low dislocation density that is, at our knowledge, at the state of the art for this material.

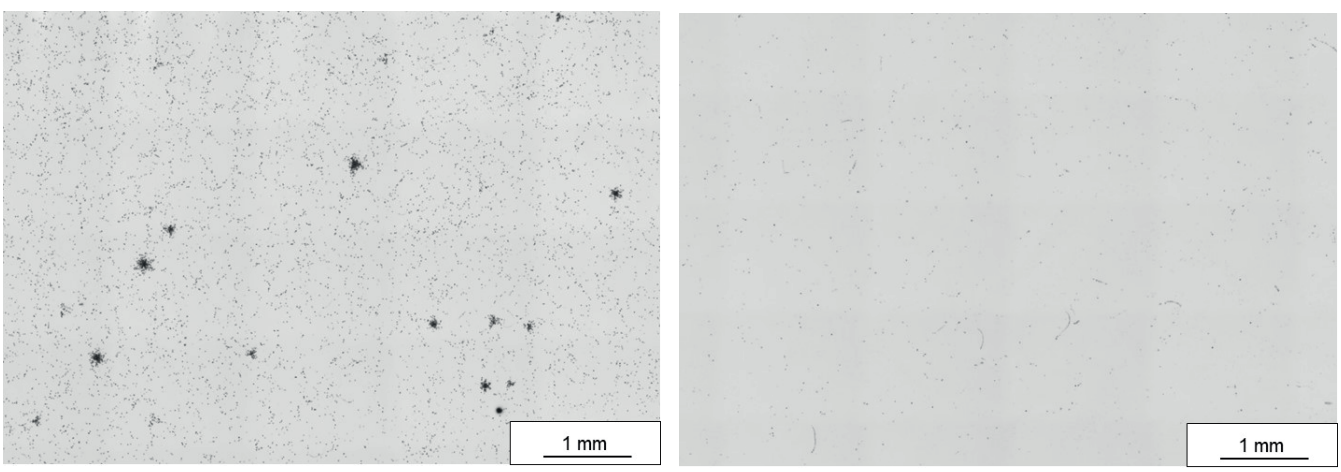

Figure 1. Etch pits observed via optical microscopy on two samples. Left: etch pit population on regular grade CdZnTe crystal (EPD ~10^4 cm^{-2}). Some clusters highlight the presence of the dislocations induced by the presence of second phase defects. The arrangement of the other etch pits seems to attest the cellular structuring of the dislocations in the crystal. Right: etch pit population on CdZnTe crystal produced with optimized process. The EPD is well below (~ 2. 10^3 cm^{-2}) and no more cluster is visible.

1. Brellier, D. *et al.* Bulk Growth of CdZnTe: Quality Improvement and Size Increase. *J. Electron. Mater.* **43**, 2901–2907 (2014).

2. Lee, D. *et al.* High-Operating Temperature HgCdTe: A Vision for the Near Future. *J. Electron. Mater.* **45**, 4587–4595 (2016).

3. Rudolph, P. Dislocation cell structures in melt-grown semiconductor compound crystals. *Cryst. Res. Technol.* **40**, 7–20 (2005).

4. Santailler, J. L. *et al.* From 5" CdZnTe ingots to high quality (111) CdZnTe substrates for SWIR 2K2 15 µm pitch infrared focal plane arrays manufacturing. in *Infrared Technology and Applications XLVI* vol. 11407 19–31 (SPIE, 2020).

Poster 08

Epitaxial growth of III-V semi-conductors on Silicon: Critical impact of the Si substrate

M. Jullien[1*], T. Rohel[1], K. Tavernier[1], A. Létoublon[1], R. Bernard[1], O. Durand[1], Y. Léger[1], N. Bertru[1], C. Cornet[1]
[1]Univ Rennes, INSA Rennes, CNRS, Institut FOTON – UMR 6082, F-35000 Rennes, France
*maud.jullien@insa-rennes.fr

The heterogeneous epitaxy of III-V semiconductors onto Si, Ge or SOI substrates has been studied for decades in the context of cost-efficient monolithic integration of photonic and energy harvesting III-V devices on silicon, including e.g. lasers, LEDs, non-linear photonic devices, photovoltaic solar cells, or photo-electro-chemical cells for solar hydrogen production. While the central importance of substrate chemical/thermal preparation prior to the III-V semiconductor epitaxy was rapidly understood [1], researchers in the field faced the lack of understanding of the very first growth steps of the III-V materials on the group IV substrate. This situation changed in 2018, with the general description of III-V on group IV (Si or Ge) epitaxy established for the first time [2]. This work, together with recent studies [3, 4] clarified especially the interplay between group IV substrate defects, substrate monoatomic coverage, miscut angle and crystal defects appearing in the epitaxially–grown III-V semiconductor.

Focusing on III-V/Si heterogeneous integration, the Si substrate preparation strategy prior to epitaxial overgrowth is always the same (in an academic Lab environment or in an industrial one). The Si substrate is first of all chemically cleaned, either with a RCA-Shiraki procedure, or a HF/oxidization one. The chemical preparation ends with a situation where the substrate surface is passivated by SiO_2 or a Si-H layer, and the sample is loaded in the epitaxial chamber (e.g. MBE or MOCVD). The substrate is then heated in situ to desorb the passivation layer (at temperatures >600°C for Si-H, and >900°C for SiO_2), and the III-V growth proceeds.

In this contribution, we detail the different issues encountered with Si substrates for III-V/Si monolithic integration. From our previous works [2-4], two key aspects of the group IV starting substrate were found to deeply impact the structural quality of the III-V/group IV samples, leading potentially to a large density of detrimental crystal defects. First, during the chemical and thermal treatment, there is a formation of small nanoscale crystallites, which generate III-V crystal twinning during the subsequent III-V epitaxy (Fig. 1 – left). Second, the use of a weak but controlled miscut (typically below 1°) is necessary to get rid of crystal defects known as “AntiPhase Boundaries” (rotation of the III-V crystal of 45° in-plane). Finally, we noticed large differences in the structural quality of III-V layers, depending on the doping nature and level of the Si substrate, and the synthesis fabrication mode (FZ vs CZ).

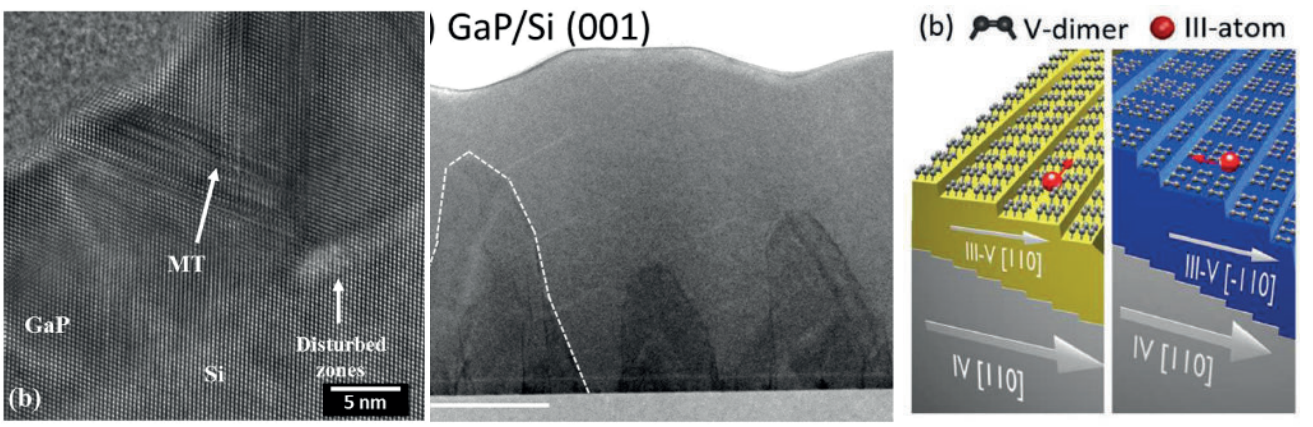

Figure 1: (left) Formation of a micro-Twin defect in a III-V layer grown on the Si substrate, from ref. [5]. The disturbed zone corresponds to the formation of crystallites at the Si substrate prior to the III-V growth. (middle) antiphase boundaries (white dashed line) and antiphase domains (darker area) appearing in the III-V semiconductor when the Si substrate miscut is not controlled (from ref.[3]). (right) The ideal situation is found when the miscut generates a regular network of steps at the Si surface, which is transferred to the III-V layers (from ref. [3]).

All these considerations and experimental findings allow us to conclude that the development of an epi-ready chemically cleaned Si or SOI substrate with a controlled miscut angle, and which could be thermally prepared at a temperature below 800°C for heteroepitaxy, would represent a key step for the development of integrated photonics or energy harvesting devices.

This work is supported by the PIANIST ANR project (ANR-21-CE09-0020), NUAGES ANR project (ANR-21-CE24-0006) and EPCIS ANR project (ANR-20-CE05-0038). The authors acknowledge RENATECH within Nanorennes for technological support.

[1] H. Kroemer, J. Cryst. Growth 81, 193 (1987).
[2] Lucci et al., Phys. Rev. Materials **2**, 060401(R) (2018).
[3] C. Cornet et al, Phys. Rev. Materials **4**, 053401 (2020).
[4] M. Rio Calvo et al., Adv. Elec. Mat. **8** (1), 2100777 (2022).
[5] Y. Ping Wang et al., Appl. Phys. Lett. 107, 191603 (2015).

Growth of 6N Purity Germanium Single Crystal Using Czochralski Technique

G.D. Patra, S.G. Singh, M. Ghosh, S.P. Pitale, A. Singh, S. Sen* L.M. Pant
Technical Physics Division, Bhabha Atomic Research Centre, Mumbai- 400085, India
**Email: shash@barc.gov.in*

Abstract*:* Germanium (Ge) Single crystals along <100> were grown using the Czochralski technique. These are the preliminary experiments to standardize parameters to grow high pure Ge for detector application. HRXRD and Hall-effect measurement (van der Pauw) measurements were studied as these are crucial parameters for the detector grade crystals.

High purity Ge (HPGe) crystals are used for the gamma ray detector [1] due to its excellent energy resolution. The growth of the pure germanium crystal is essential, especially for nuclear detector application. Germanium is also finds many applications in waveguides, infrared (IR) window fibre optics, space solar cells and as polymerization catalysts [2]

Experiments: Single crystals of germanium are grown by the Czochralski technique. Initial charge was obtained from, Umicore, Belgium with 6 N pure in 40mm bar form. The schematic of growth station is shown in Fig.1. It consists of a quartz crucible inside a graphite susceptor. Bar of germanium were taken in the quartz crucible of 110 mm diameter and 100 mm length. Before loading into the crucible, raw materials were etched with $1HF:3HNO_3$ mixture solution to remove any contamination on the surface and rinsed with deionized water 2–3 times, and dried by nitrogen gas. Seed used was oriented in <100> directions and were cleaned by the same procedure.

Germanium was melted by heating with the help of a 50 kW RF furnace in pure argon environment. A continuous argon flow of 0.5l/min was maintained during the growth. Temperature of melt was raised by 50 ºC above melting temperature (937 ºC) then was slowly lowered to achieve the growth temperature (super cooled melt). A typical rotation rate of 15-20 rpm and a pull rate of 15-25 mm/h were used during the growth of Ge single crystal of 50 mm diameter and 120 mm length. The growth experiments were carried out in class-100 clean room while material preparation was done in class-1000 clean environment.

After growth, 2 mm thick discs were cut from top, middle and bottom of the crystal using low speed diamond saw and polished to roughness of 0.5 µ. Single Crystal quality was checked by high resolution XRD. Carrier concentrations and resistivity were measured Hall Effect measurement system within a range of temperatures from 77K to 300K.

Results and Discussion: Single crystals of germanium of 50 mm diameter and 120 mm length were grown. A typical photograph of an as-grown crystal is shown in Fig 2. 100% charge was pulled in the form of single crystal in each growth to avoid the cracking of the quartz crucible. Apparently grown crystal was crack free and HRXRD performed in the top part of the crystals show good of the crystalline lattice quality with a FWHM of 90 arc sec.

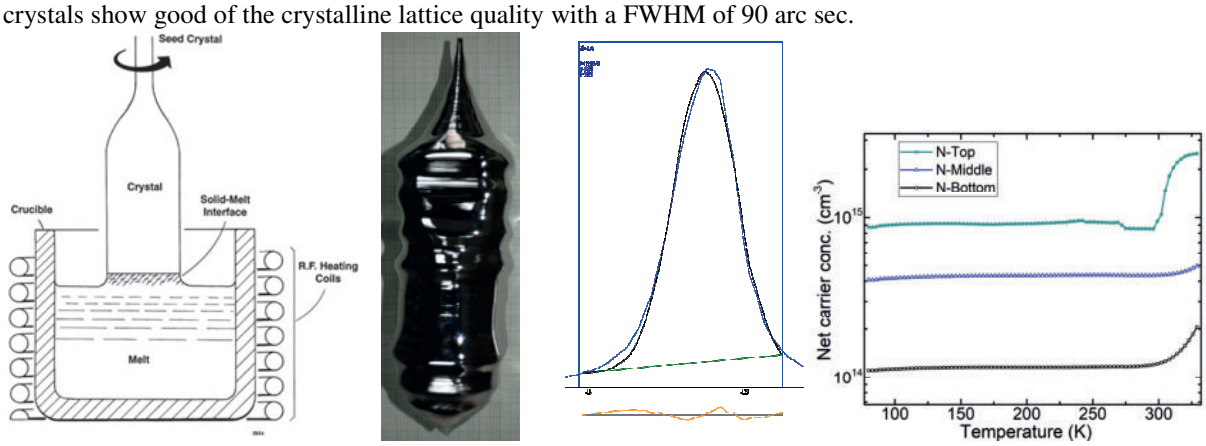

FIGURE 1. Schematic of growth station used for single crystal growth of germanium. **2.** A typical photograph of as grown crystal. **3.** XRD rocking curve of crystalline germanium (400) **4**. Temperature-dependent net carrier concentration of germanium crystal.

In Hall measurement, resistivity for all the parts of crystals are below 20 ohm.cm^{-1} in 77 k-300k.The crystal is N-type and the top part of the grown crystal exhibits a net carrier concentration $\approx 10^{13}$cm^{-3} that gradually descends to $\approx 10^{15}$ cm^{-3} at the bottom at 80 K. This infers that during crystal growth no further impurity are added and resulted crystal is better than 6N.

Conclusion: Single crystal of germanium along <100> orientation have been grown successfully as a preliminary experiment.

REFERENCES

1. R.N. Hall, *Semiconductor Materials for Ggamma Ray Detectors* (Proceedings of meeting 24 June 1965) edited by W.L. Brown and S. Wagner, P.27.
2. E.E. Haller, W.L. Hansen, F.S. Gaulding, *Advances in Physics* **30**, 93-138 (1981).

Poster 10

Crystal growth, morphology, and luminescence properties of LuSAG:Tm single crystals

J. Pejchal[1], J. Havlíček[1,2], J. Šulc[3], K. Nejezchleb[2], H. Jelínková[3]

[1] Institute of Physics AS CR, Cukrovarnická 10, Prague, 16200, Czech Republic

[2] Crytur Ltd., Na Lukách 2283, Turnov, 51101, Czech Republic

[3] Faculty of Nuclear Sciences and Physical Engineering, Czech Technical University, Trojanova 13, Prague, 12000, Czech Republic

E-mail: pejchal@fzu.cz

Tm-doped multicomponent laser crystals are intended for 2 μm laser generation [1]. Due to the disordered structure of these crystals, the absorption and emission lines of thulium ions are significantly spectrally broadened, which is advantageous both for efficient diode pumping and for wide laser tunability or for the generation of very short pulses in mid-infrared spectral region. Possible applications of such lasers include medical applications, high-resolution spectroscopy, and remote sensing [1].

We have prepared the Tm-doped multicomponent $Lu_3Sc_1Al_4O_{12}$ single crystals with different Tm concentrations by the micro-pulling-down method [2, 3] using two types of crucibles. One was a classical crucible with 3 mm diameter circular shaped die with one 0.5 mm capillary. The crystals could be grown well without cracks or any visible inclusions; see example in Fig. 1. However, observations with a microscope under polarized light showed significant inhomogeneities, deteriorating the optical properties of samples. Therefore, we have changed the crucible design in a way that the 3 mm diameter die included a 2 mm diameter orifice conically widened downwards. Such a design led to crystal homogeneity improvement and the resulting positive influence on the optical properties.

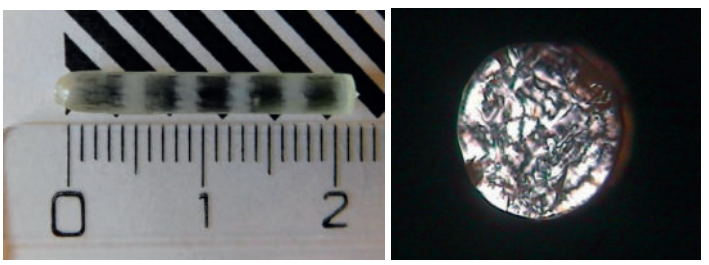

Figure 1. Single crystal of Tm 4% -doped $Lu_3Sc_1Al_4O_{12}$ grown by the micro-pulling-down method (left) and its cross-section in the microscope observed with polarized light.

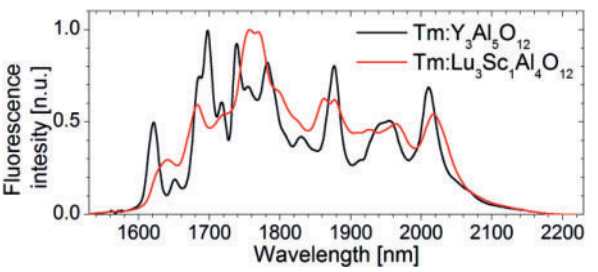

Figure 2. Comparison of Tm 4%-doped $Lu_3Sc_1Al_4O_{12}$ and in $Y_3Al_5O_{12}$ fluorescence spectra corresponding to $^3F_4$ -> $^3H_6$ transition under 0.8 um excitation.

The fluorescence spectra of Tm-doped $Lu_3Sc_1Al_4O_{12}$ in comparison with Tm-doped $Y_3Al_5O_{12}$ are shown in Fig. 2. The details and peculiarities of the crystal growth and crucible design and preliminary luminescence studies of this material system will be presented and discussed.

References:

[1] Walsh, B.M. Review of Tm and Ho materials; spectroscopy and lasers. Laser Phys. 19 (2009) 855

[2] A. Yoshikawa, M. Nikl, G. Boulon, T. Fukuda, Challenge and study for developing of novel single crystalline optical materials using micro-pulling-down method, Optical Materials 30 (2007) 6–10

[3] A. Yoshikawa, V. Chani, Growth of Optical Crystals by the Micro-Pulling-Down Method, MRS Bulletin 34 (2009) 266–270

Numerical study of dislocation density distribution in silicon crystals under different temperature conditions

A. Sabanskis[1*], K. Dadzis[2], L. Vieira[2], R. Menzel[2], and J. Virbulis[1]

[1]Institute of Numerical Modelling, University of Latvia, 3 Jelgavas Street, LV-1004 Riga, Latvia

[2]Leibniz-Institut für Kristallzüchtung, Max-Born-Str. 2, 12489 Berlin, Germany

*Presenting author's e-mail: andrejs.sabanskis@lu.lv

The generation and multiplication of dislocations in silicon (Si) single crystals is strongly affected by the thermal stress level. While generation of dislocations is considered the main cause for process failure during growth of Si single crystals, existing numerical models cannot precisely predict this phenomenon. To better understand the dislocation origins and their behaviour at different temperatures, a model experiment [1] has been carried out at the Leibniz Institute for Crystal Growth (Berlin). During the experiment, different sections of a floating zone (FZ) Si single crystal (diameter 20 mm, length 480 mm) were heated by a high-frequency (HF) inductor to temperatures from 700°C up to 1180°C, but still below the melting point of Si (1414°C). After the crystal cooled down to room temperature, it was cut and dislocation distributions at different cross-sections were analysed. A well-defined initial appearance of dislocations was observed at about 995°C.

Numerical simulations of the transient temperature field and dislocation density dynamics in the above-mentioned experiment [1] were carried out in [2]. A very good agreement with experiment was achieved for the temperature field. The dislocation density dynamics were modelled with the Alexander-Haasen (AH) model [3] which was extended with a temperature-dependent critical stress threshold to better describe the initial dislocation appearance observed in the experiment. As depicted in Figure 1, the local increase in dislocation density at crystal sections and the extension of the dislocated zone from the crystal side surface were correctly predicted by the simulations, however, dislocations near the crystal axis were not captured by the AH model, possibly, due to neglected effect of dislocation propagation.

In the present contribution, further numerical simulations using the previously developed model system and the corresponding open-source solver package MACPLAS [2,4] are carried out. Furthermore, another model was developed in COMSOL Multiphysics to provide input boundary conditions for the crystal surface, such as the induced heat sources, thermal radiation, and convective heat losses. The parameters related to crystal heating are varied to investigate the effects of the stress and temperature fields on the final dislocation density distribution:

- A toroidal graphite susceptor is considered between the inductor and the crystal. It is tested whether a less localized heating due to radiation of the susceptor would reduce the stresses to obtain a dislocation-free crystal;
- Heat pulses are investigated using transient simulations. It is tested whether dislocations would be created at relatively low temperatures in the presence of especially high stress gradients.

Based on the simulation results, suggestions for possible further experiments are formulated.

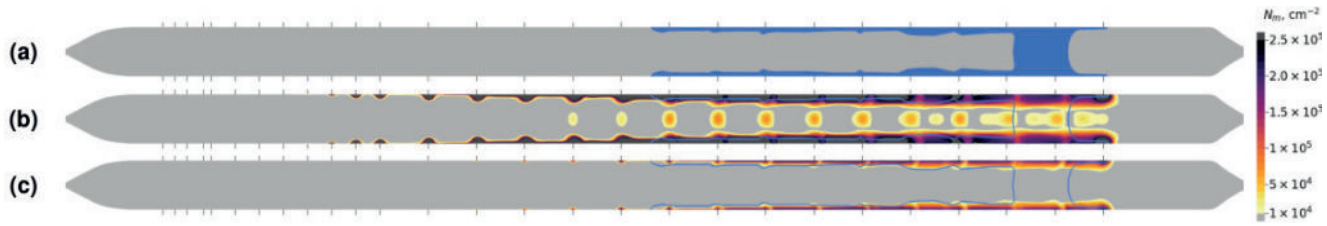

Fig. 1. Shape of dislocated zone in experiment (a); calculated dislocation density [2] without (b) and with critical stress threshold (c). Experimentally observed boundary of the dislocated zone is depicted in (b,c) as blue curves; black horizontal lines show heating positions at which the crystal is not moving. The heating direction is from left to right.

Acknowledgements

The present research has been supported by the PostDoc Latvia Project No. 1.1.1.2/VIAA/2/18/280.

References

1. H.-J. Rost, I. Buchovska, K. Dadzis, U. Juda, M. Renner, R. Menzel. Thermally stimulated dislocation generation in silicon crystals grown by the Float-Zone method. Journal of Crystal Growth, vol. 552 (2020), p. 125842.
2. A. Sabanskis, K. Dadzis, R. Menzel, J. Virbulis. Application of the Alexander–Haasen model for thermally stimulated dislocation generation in FZ silicon crystals. Crystals 12, no. 2 (2022), 174.
3. H. Alexander, P. Haasen. Dislocations and plastic flow in the diamond structure. Solid state physics, vol. 22 (1969), pp. 27-158.
4. MACPLAS: MAcroscopic Crystal PLAsticity Simulator. Available online: https://github.com/aSabanskis/MACPLAS.

Poster 12

High Energy Computed Tomography as a Tool for Validation of Numerical Simulations of Ammonothermal Crystal Growth of GaN

S. Schimmel[1,*], M. Salamon[2], D. Tomida[3], T. Ishiguro[4], Y. Honda[3], S.F. Chichibu[3,4], H. Amano[3]

[1]Friedrich-Alexander-Universität Erlangen-Nürnberg, Crystals Growth Lab, Materials for Electronics and Energy Technology (i-MEET), Martensstraße 7, 91058 Erlangen, Germany
[2]Fraunhofer IIS, Fraunhofer Institute for Integrated Circuits IIS, Division Development Center X-Ray Technology, 90768 Fürth, Germany
[3]Institute of Materials and Systems for Sustainability, Nagoya University, Nagoya 464-8601, Japan
[4]Institute of Multidisciplinary Research for Advanced Materials, Tohoku University, Sendai 980-8577, Japan
[*]saskia.schimmel@fau.de

The ammonothermal method is recognized for providing GaN seeds of excellent structural quality and as a tool for exploratory nitride synthesis(1). Due to its capability to grow many crystals simultaneously, it can not only serve as a seed provider for hydride vapor phase epitaxy (HVPE) but may also become a strong competitor for HVPE after further scale-up(2). Efficient scale-up of bulk growth of GaN and the method's application to further materials would equally benefit from numerical simulations of the growth process. For scale-up, numerical simulations have the potential to efficiently tailor conditions of temperature, fluid flow and supersaturation field when transitioning to larger reactors. Likewise, the fundamental understanding that is required for sufficiently accurate simulations would significantly accelerate the development of growth processes also for emerging materials.

However, numerical simulations of ammonothermal growth are at an immature stage of development and a clear understanding of their accuracy is missing, which is largely due to a lack of experimental access for validation(3). In particular, a method for tracking Ga mass transport throughout the entire inner volume of an ammonothermal autoclave would be a valuable addition to in situ monitoring technology. X-ray imaging using moderate x-ray energies up to 100 kV can be used for tracking Ga transport and GaN dissolution(4), however, this approach yields insight only into a limited fraction of the inner volume of an autoclave because ceramic windows with a limited area of view need to be used.

To access the full inner volume, it is necessary to use a technology that can penetrate the metallic walls of the high-pressure autoclave. High energy computed tomography (CT) has previously been applied for studying crystal growth kinetics in physical vapor transport(5), however, the absorption of an ammonothermal growth setup is different. The absorption by the nickel-base alloy autoclave wall has a large impact. To clarify whether in situ CT can be established as a tool for monitoring mass transfer of Ga during ammonothermal crystal growth, it is therefore necessary to investigate the specific case. In particular, a dedicated investigation is necessary for estimating the achievable resolution in time and space, as well as for identifying suitable photon energies that yield a good combination of x-ray transmission and contrast. Ex situ CT measurements with a complete ammonothermal setup are shown in Figure 1.

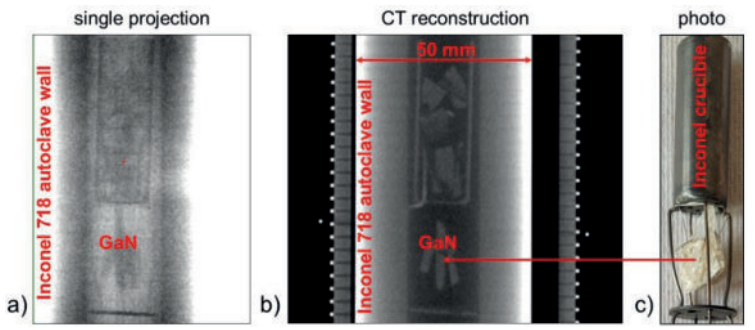

Figure 1 Computed tomography conducted ex situ, i.e. with ambient air instead of the ammonothermal reaction medium inside the autoclave: a) Single projection image, b) CT reconstruction, c) photograph of setup that was placed inside the autoclave for the CT measurements. All x-ray images were obtained at an acceleration voltage of 600 kV and with 1 s exposure time for a single projection. The reconstruction is based on 1200 single projections recorded at different angles within a total measurement duration of 20 minutes.

Ex situ computed tomography measurements will be analyzed with regard to the technique's applicability for tracking mass transfer. Key challenges inherent to numerical simulations of temperature and fluid flow inside ammonothermal autoclaves will be outlined, in part based on exemplary numerical results. Prospects and challenges of applying computed tomography as a tool for validation of numerical simulations of GaN growth will be analyzed.

References

(1) J. Häusler, W. Schnick, Chemistry – A European Journal, 24 (2018) 11864-11879.
(2) R. Kucharski, T. Sochacki, B. Lucznik, M. Bockowski, J. Appl. Phys., 128 (2020).
(3) S. Schimmel, D. Tomida, T. Ishiguro, Y. Honda, S. Chichibu, H. Amano, Crystals, 11 (2021).
(4) S. Schimmel, P. Duchstein, T.G. Steigerwald, A.C.L. Kimmel, E. Schlücker, D. Zahn, R. Niewa, P. Wellmann, J. Cryst. Growth, 498 (2018) 214-223.
(5) M. Arzig, M. Salamon, N. Uhlmann, P.J. Wellmann, Advanced Engineering Materials, 22 (2019).

Effect of Co-doping in the growth and scintillation performance of $CeBr_3$

D. S. Sisodiya[1, 2], S. G. Singh[2], G. D. Patra[2], Shashwati Sen[*1,2]
[1]Homi Bhabha National Institute, Mumbai 400094 India.
[2]Technical Physics Division, Bhabha Atomic Research Centre, Mumbai 400085, India
*shash@barc.gov.in

Scintillator detectors plays an important role in isotope identification and has application in nuclear medicine and homeland security. $CeBr_3$ and $LaBr_3$: Ce are the advanced scintillators in terms of performance and have ability to replace Tl-Doped CsI and NaI. The commercial availability and application of these lanthanide halide's is limited because their mechanical properties, which are not suitable for growth of large sized crack free single crystal, hygroscopicity of material and the tendency of multi orientation growth. $CeBr_3$ has an asymmetrical hexagonal UCl_3 type crystal structure with a $P6_3/m$ space group with non-isotropic expansion coefficient [1] which leads to cracking during the cooling period of crystal growth. Aliovalent doping is the best suitable tool for providing the strength to the single crystal of $CeBr_3$ [2], here selection of doping is specific it should not degrade the scintillation performance [3].

We have grown $CeBr_3$ single crystal with Ca^{2+} and Ba^{2+}, and also co-doped with both dopants with different concentrations by vertical Bridgman technique. To inhibits the multi orientation nucleation a crucible with grain selector was designed and used. The single crystal growth was carried out in six zone Bridgman furnace. The detail of crystal growth experiment and design of crucible is given on another paper [3]. Previously we have observed that Ba^{2+} doping reduces the hygroscopicity of $CeBr_3$ and a small enhancement in the scintillation performance compare to pure one [3].

We recorded a 4.2 % Energy resolution for $CeBr_3$ crystal co-doped with 0.25% Ba^{2+} and 0.25% Ca^{2+} at 662 KeV for ^{137}Cs gamma source (Figure 1.) and there is an increment in light yield as compare to pure one and individual doping of Ba^{2+} and Ca^{2+}. It has also been observed that Ba^{2+} doping helps in the growth of crack free large size $CeBr_3$ single crystal when its doping percentage is higher as compare to the second dopant.

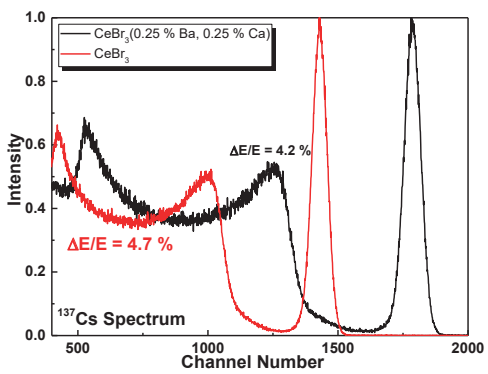

Figure 1. Gamma Ray spectra for ^{137}Cs of Pure $CeBr_3$ and co-doped $CeBr_3$

Acknowledgements

Authors wish to thank all Crystal Technology Lab (Bhabha Atomic Research Centre, Mumbai) for their support and assistance during the crystal growth and crystal processing.

References

1. F. G. A Quarati, et al. "Scintillation and detection characteristics of high-sensitivity CeBr3 gamma-ray spectrometers." Nuclear Instruments and Methods in Physics Research Section A: Accelerators, Spectrometers, Detectors and Associated Equipment 729 (2013): 596-604.
2. Paul Guss, et al. "Results for aliovalent doping of CeBr3 with Ca2+." Journal of Applied Physics 115.3 (2014): 034908.
3. D. S. Sisodiya, et al. "Effect of Ba^{2+} Doping on the Properties of CeBr3 Single Crystal." Journal of Crystal Growth (2022): 126528.

Growth, structural and optical properties of $Gd_2Ti_2O_7$ single crystals

M Suganya[1], K.Ganesan[2], P Vijayakumar[2], Amirdha Sher Gill[3], R.M. Sarguna[2], A. Edward Prabu[2], S.Ganesamoorthy[2] and S.Moorthybabu[1]
[1]Crystal Growth Center, Anna University, Chennai, Tamilnadu, India;
[2]Materials Science group, IGCAR, Kalpakkam, Tamilnadu, India;
[3]Sathyabama Institute of Science of Technology, Chennai, Tamilnadu, India
E-mail: suganyatvmalai29@gmail.com & sgm@igcar.gov.in

The $Gd_2Ti_2O_7$ is one of the technologically important materials with diverse applications including photocatalyst, ionic conductivity, host material for optical emission and nuclear waste immobilization. Since many of the physical and chemical properties of GTO emerge from the oxygen off-stoichiometry, the study on structure – property correlation is indispensable. In this study, $Gd_2Ti_2O_7$ single crystals were grown by optical floating zone technique under different growth atmospheres such as oxygen, air and argon. The color of the crystals grown in O_2, air and Ar is found to be light amber, dark amber and black, respectively. The growth of $Gd_2Ti_2O_7$ single crystals in O_2 is challenging because the stability of molten zone was heavily disturbed by continuous bubble formation which can lead to catastrophic failure of growth by detachment of feed/seed rods. Moreover, the crystals grown in air had developed a lot of cracks which prohibits the large size wafer preparation. On the other hand, a uniform diameter and crack-free crystals could be easily grown in Ar atmosphere, although the grown crystals are completely opaque to light due to oxygen vacancies. The structural and optical properties of the as-grown and annealed crystals are studied systematically using XRD, Raman, UV-Vis and photoluminescence spectroscopy. The full width at half maximum of X-ray diffraction rocking curve decreases from 245 to 157 arc-second and the optical transmittance increases from 23 to 87 % (at 1000 nm) upon post growth thermal annealing. Raman spectroscopic studies reveal a monotonic increase in intensity of O-Gd-O (E_g) and Ti-O (A_{1g}) stretching modes with thermal annealing. The increase in Raman intensity indicates an improvement in structural ordering of oxygen sub-lattice in $Gd_2Ti_2O_{7-\delta}$. Moreover, the photoluminescence studies also corroborate the Raman analysis in terms of reduction of structural defects associated with oxygen vacancies as a function of thermal annealing.

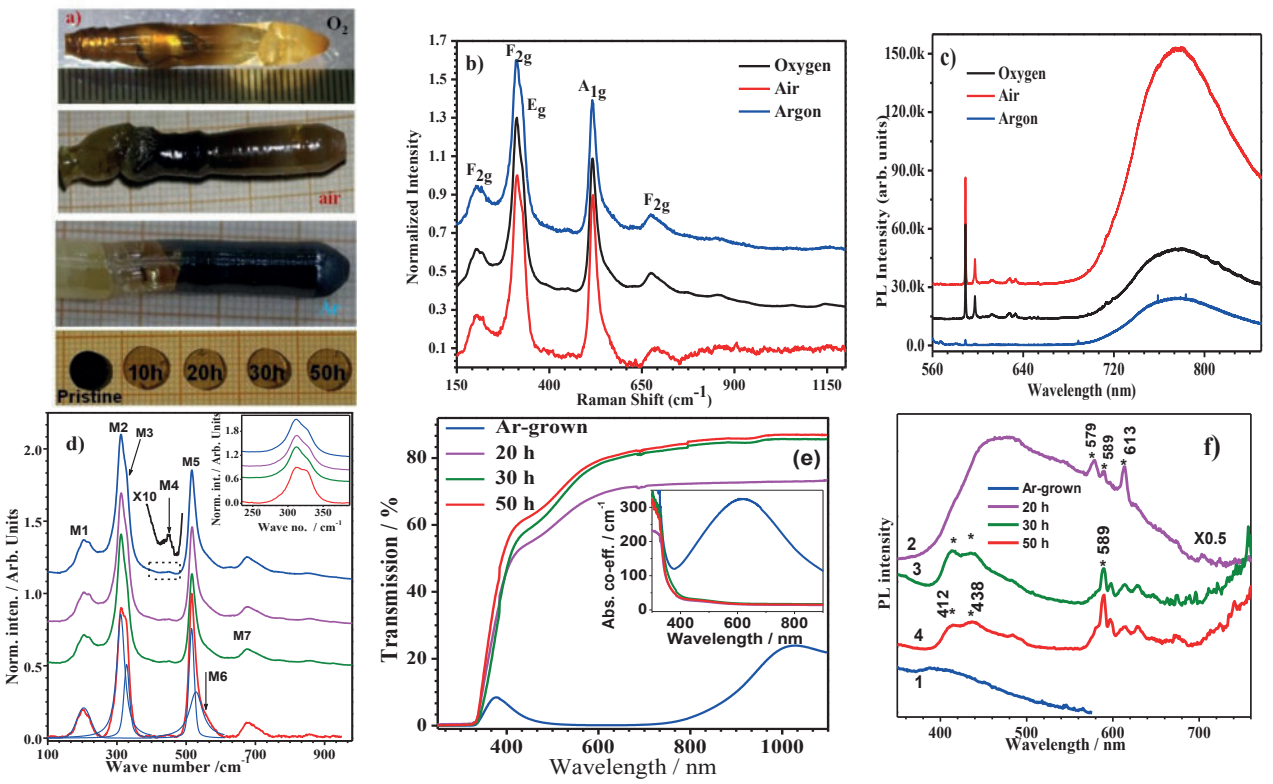

Fig 1 a) $Gd_2Ti_2O_7$ single crystals grown in O_2, air and Ar atmosphere and their respective (b) Raman and (c) PL spectra. The (d) Raman, (e) UV-Vis and (f) PL spectra of GTO crystals (grown in Ar) that are annealed at 1000 ^{O}C for different durations.

Investigations on n-Type Doping on OFZ Grown Beta-Gallium Oxide Single Crystals for Power Device Applications

Vijayan Ananthu[1], Kaza Venkata Akshita [1], Dhandapani Dhanabalan [1],Rajendran Hariharan[1], Sridharan Moorthy Babu[1]

[1] Crystal Growth Centre, Anna University; Chennai, INDIA;
anugwri@gmail.com, smoorthybabu@gmail.com

β-Ga_2O_3 is an ultra-wide bandgap (~4.8eV) semiconductor widely used in power electronics and optoelectronic devices which operates in shorter wavelength. Under normal conditions, it behaves like an insulator, due to the ultra-wide bandgap of this material. It becomes an n-type semiconductor under reduced conditions. The conductivity is mainly due to the oxygen deficiencies in the crystal lattice. Single crystals of both undoped, Sn and Ta doped β-Ga_2O_3 were grown by using optical floating zone technique. By n-type doping the resistivity can be controlled down to 10 mΩ/cm. Sn has been the most widely investigated as a promising dopant for gallium oxide. When Sn substitutes for Ga^{3+} on the octahedral site in a 4^+ oxidation state, it donates an electron to the Ga_2O_3 lattice, which increases the carrier concentration and thus conductivity. The rate and direction of rotation of seed rod and feed rod control stirring of molten material which influence the temperature distribution and composition within the molten zone. Initially, grown crystals exhibits twin boundary defects and many cleavage planes. Later by several trial-and-error methods, the growth parameter such as rotation of both feed and seed rod was set as 15-20 rpm and translation as 5-9 mm/hr were optimized. The grown crystals (fig.1.) were subjected to wafer processing steps such as slicing, grinding and polishing. The quality of the crystals was analyzed by HR-XRD and single crystal XRD. From Single crystal XRD (Fig.2.) data, the monoclinic structure of β-Ga_2O_3 is changed to triclinic due to the larger ionic radius of Sn. Several studies such as spectroscopic, electrical, optical, mechanical and surface morphological were performed on the wafers. XRD plot (Fig.3.) shows all the crystals were in (010) orientation. From the UV-Vis spectroscopy, the transmittance of all wafers were above 80%. The vibrational modes presented in the wafers were confirmed using Raman spectroscopy (Fig.4.). Also there is a blue shift due to the incorporation of Sn. Surface roughness of the wafer has been confirmed with AFM micrographs (Fig.6.). The roughness is ~2-3 nm, which is suitable for device fabrication. Current focus is on fabricating power electronics using Sn doped gallium oxide wafers.

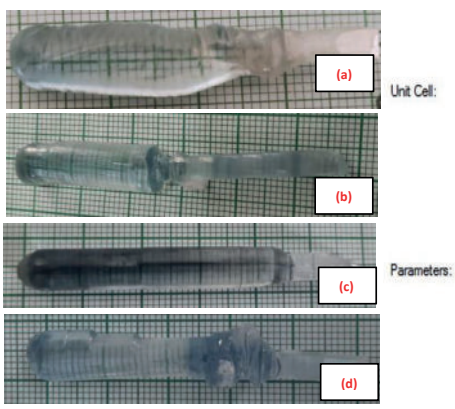

Fig. 1. As grown Ga_2O_3 single crystal (a)Undoped. (b) 0.05%. (c) 0.1%. (d) 0

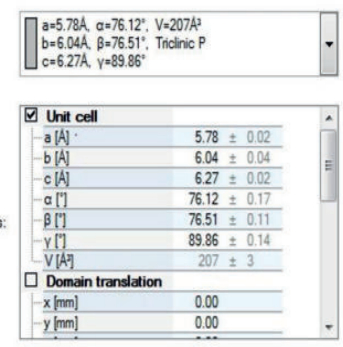

Fig. 2. Single crystal XRD :Unit cell parameters for Sn:Ga_2O_3.

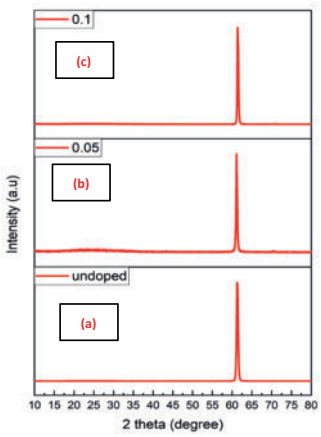

Fig.3. XRD plot (a)Undoped. (b) 0.05%. (c) 0.1%. (d) 0.2%.

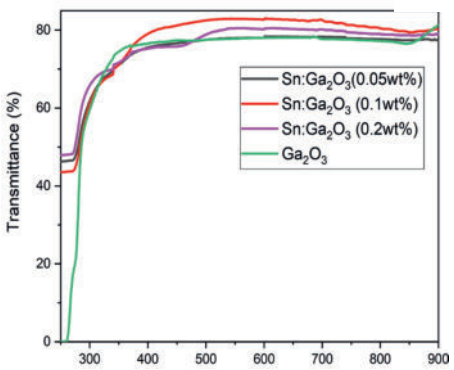

Fig.4. UV- Vis Transmission spectra of undoped and Sn doped Ga_2O_3 single crystals.

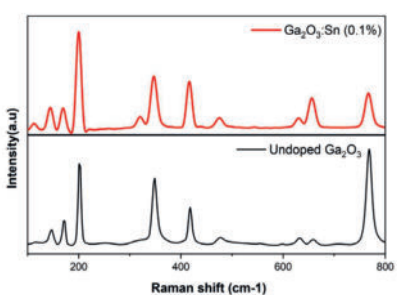

Fig.5. Raman spectra of undoped and Sn doped Ga_2O_3 single crystals.

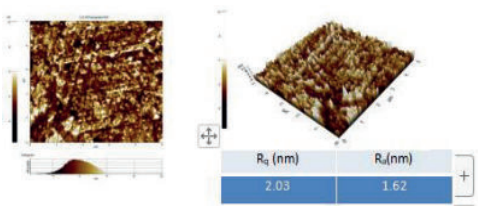

Fig.6.Roughness measurement using AFM

Growth and Characterization of $Tb_3Ga_5O_{12}$ Single Crystals

Miki Watanabe*[1,2], Takeshi Hayashi[1], Yutaka Anzai[1], and Isao Tanaka[2]

[1] OXIDE corporation, 1747-1 Makihara, Mukawa, Hokuto, Yamanashi 408-0302, Japan

[2] University of Yamanashi, Miyamae 7-32, Kofu, Yamanashi 400-0021, Japan

*E-mail: miki.watanabe@opt-oxide.com

【Introduction】

$Tb_3Ga_5O_{12}$ (TGG) single crystals have excellent characteristics for optical isolator such as high-Verde constant, high-thermal conductivity and low-optical loss. However, TGG single crystals grown by the Czochralski (Cz) method have radial stripe patterns (called striae) besides crystal defects such as cores and voids, as shown in Fig. 1. In this study, we examined the mechanism of striae in TGG single crystals, and optimized the growth conditions to grow striae-free TGG single crystals.

【Experiments and results】

TGG single crystals were grown along <111> by the Cz method using a high-frequency induction heating. The grown crystals were cut parallel to the growth direction, and mirror-polished. The striae in the TGG grown crystals were characterized by polarizing microscopy and etching method. In the crossed Nicol state of the polarizing microscope, striae with several hundred micrometers width were observed orthogonal to the growth striations. In the sample etched in phosphoric acid at 170 ℃, the etch pits were observed along the boundaries between the striae and the TGG matrix, as shown in Fig. 2. The array state of the etch pits suggests a huge helical dislocation as similar defects had been reported in $Gd_3Ga_5O_{12}$ single crystals.[1-2] Also, a typical pattern due to the helical dislocations were confirmed by X-ray topography. The origin of the helical dislocations may be due to a non-uniform solidification by a constitutional supercooling. We focused on the relationship between the constitutional supercooling and off-congruent melting behavior. The congruent-melting composition was evaluated by measuring the lattice constant of the grown TGG single crystals. The lattice constant was constant along the growth direction of the crystals grown from congruent melt. As a result, striae-free TGG single crystals were grown successfully.

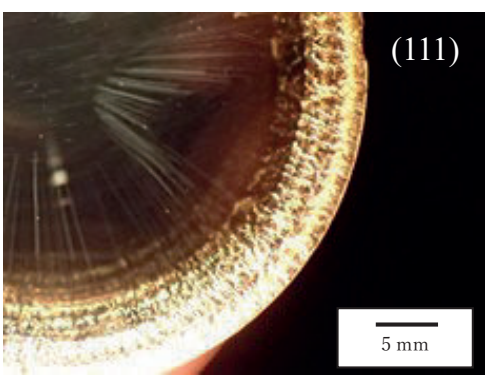

Fig. 1 Radial stripe patterns (striae) of the cross section in TGG single crystal.

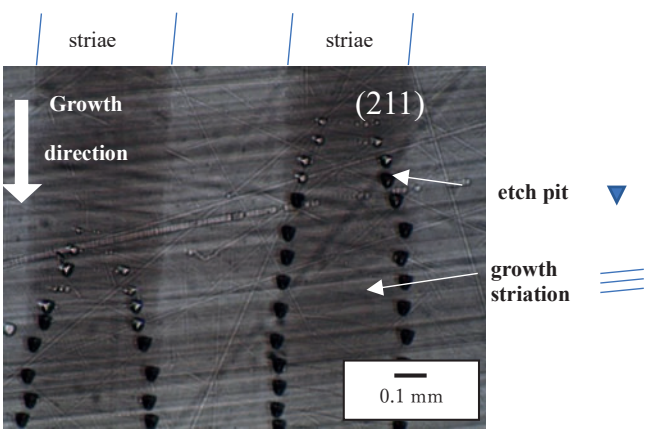

Fig. 2 Elliptical etch pits of the longitudinal section in TGG single crystal.

References

[1] Y. Imamura and S. Shinoyama, Jpn. J. Appl. Phys. **13** (1974) 379-380.

[2] K. Takagi, T. Fukazawa and M. Ishii, J. Crystal Growth **36** (1976) 185-187.

Poster 17

In-band pumped Ho:CALGO crystal for efficient high-power laser operation at 2.1 µm

Weichao Yao[1], Yicheng Wang[1], Christoph Liebald[2], Daniel Rytz[2], Volker Wesemann[2], Klaus Dupré[2], Daniel Dümichen[2], Tamara Berzen[2], Mark Peltz[2], Clara J. Saraceno[1]

[1]*Photonics and Ultrafast Laser Science, Ruhr Universität Bochum, Universitätsstrasse 150, 44801 Bochum, Germany*
[2]*Electro-Optics Technology GmbH, Struthstraße 2, 55743 Idar-Oberstein, Germany*

E-mail: weichao.yao@ruhr-uni-bochum.de

Broadband solid-state lasers directly emitting at 2.1 µm that can potentially achieve high average power, ultrashort pulses are an important topic of research due to growing demands in spectroscopy, polymer processing, and for efficiently driving secondary sources from the THz to the XUV. In order to reach the desired performance, Ho^{3+}-doped laser gain media are one attractive alternative, but the gain material requires both high thermal conductivity and a broad gain spectrum simultaneously, which is known to be very challenging. Disordered $CaLnAlO_4$ (Ln stands for Gd/Y/Lu) crystal can provide high thermal conductivity (6.7 $Wm^{-1}K^{-1}$) and nearly 100 nm of gain band width when it is doped with Ho^{3+} [1]. Furthermore, Yb:$CaLnAlO_4$ has shown remarkable performance at 1 µm [2]. However, so far, only a few laser results are reported based on Ho:$CaYAlO_4$ [3]. No reports were made of laser operation or mode locking of Ho:$CaGdAlO_4$. In this paper, we present first achieved results in this direction with Ho:$CaGdAlO_4$, showing first CW operation with high-power in the bulk geometry.

The Ho:CALGO crystal (3.1 at.% doping concentration) was grown in a Φ80 mm Ir-crucible after already one boule has been grown from the melt. Doping concentration was adjusted between both growth runs and raw material powder in the amount of the precursor crystal's weight was added. The pulling speed and crystal rotation were set to 0.7 mm/h and 15 RPM, respectively. The crystal used in these first experiments was 15 mm long, and cut at Brewster's angle for access to π-polarization, which corresponds to higher absorption and laser gain [1]. We first tested the crystal in CW operation. Figure 1a shows the schematic of the laser setup, which is already designed for future mode locking experiments. A single-mode 1940-nm Tm-fiber laser was used as the pump source. Small-signal absorption of the crystal for the pump light was estimated to be ~80%. The laser output power was tested with four OCs with different transmissivity T_{OC}, as shown in Fig. 1b. The output power shows a linear dependence on the absorbed pump power. A maximum output power of 2.7 W was achieved at 7.6 W absorbed pump power with T_{OC} = 5%, with a slope efficiency of 44.6%. The laser wavelength has a significant blue shift with the increase of T_{OC}, see Fig. 1c. To further study the wavelength tunability of the crystal, a 5-mm thick quartz birefringent filter was placed in the cavity at Brewster angle. With T_{OC} = 5%, 80-nm tuning range from 2068 to 2120 nm was obtained at 4.5-W absorbed pump power, indicating that the Ho:CALGO crystal can support sub-100 femtoseconds pulse widths.

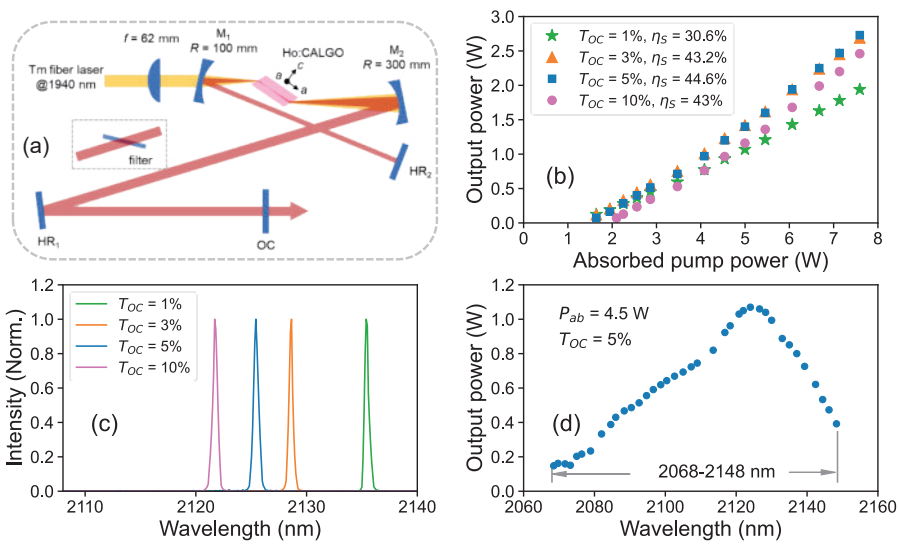

Fig. 1. Experimental setup (a), laser output power (b) and wavelength (c) with different T_{OC}, and wavelength tunability (d) of the Ho:CALGO laser.

[1] Y. Wang, P. Loiko, Y. Zhao, Z. Pan, W. Chen, M. Mero, X. Xu, J. Xu, X. Mateos, A. Major, M. Guina, V. Petrov, and U. Griebner, Opt. Express 30(5), 7883-7893(2022).
[2] W. Tian, R. Xu, L. Zheng, X. Tian, D. Zhang, X. Xu, J. Zhu, J. Xu, and Z. Wei, Opt. Lett. 46(6), 1297-1300(2021).
[3] D. Zhou, J. Di, C. Xia, X. Xu, F. Wu, J. Xu, D. Shen, T. Zhao, A. Strzęp, W. Ryba-Romanowski, and R. Lisiecki, Opt. Mat. Express 3(3), 339-345(2013).

Solid-State Microwave Generators at 2.45 GHz for Microwave Plasma Assisted CVD and ALD Processes

G. Hintz[1], V. Ramopoulos[1], J. Schlundt[1], S. Wassenberg[1], R. Heilig[1] and M. Schweizer[1]
[1] *TRUMPF Hüttinger, Germany*
gerd.hintz@trumpf.com

1. Introduction

Single-crystalline high purity synthetic diamonds are increasingly used for various applications. With the growing number of high-tech applications, the need for larger diamonds and other carbon materials (e.g. graphene) arises. Here, the classical manufacturing processes based on Microwave Plasma Assisted Chemical Vapour Deposition (MW-CVD), which are based on magnetron driven systems, reach their limits. The limits are set by the operating frequency of the respective applicator since the diameter of the possible plasma area is limited to λ/2. Therefore, there is a need to investigate new approaches to generate larger-area homogeneous microwave-driven plasma. One promising approach seems to be the replacement of the classical magnetron by modern microwave solid-state power generators (MW-SSPGs). This opens a new world through their simple frequency, amplitude and phase tunability. In this context TRUMPF Hüttinger has developed an innovative MW-SSPG product series, which is described in more detail below.

2. Features and USPs of TRUMPF Hüttinger's MW-SSPG

The key element of all TRUMPF Hüttinger's MW-SSPG, *TruPlasma MW series*, at 2.45 GHz is a 300-Watt pallet (amplifier) module. Each pallet is serially equipped with an integrated circulator, this allows a reflected power of 150% for 60 seconds to be sustained. The individual pallets are equipped with GaN transistors, which enable an outstanding power efficiency of up to 65% at module level. Based on this ultra-robust and innovative modules, larger power classes of currently up to 8 kW at 2.45 GHz can be realized by a special power combining process adapted to the generators. Furthermore, the *TruPlasma MW series* generators are equipped with integrated power sensors for forward and reflected power measurement and a very fast control unit developed in-house. Combined with a very advanced software, which allows their control through EtherCat in real time and Ethernet, several special features can be enabled. a) Due to the generator's ability to switch within 1 ms between different frequencies, the generator can independently scan the entire ISM band between 2.4 and 2.5 GHz and identify all possible resonances within the MW applicator, with each resonance within a resonator associated with a different field pattern/mode. Thus, by optimizing the combination of multiple field patterns, much higher field homogeneity/plasma homogeneity can be achieved over an area >> λ/2. b) In case of multi-generator system, by varying the phase dependencies between the generators, an increased/controlled plasma homogeneity can be achieved even in case of increased plasma density. c) By providing ultrashort pulses of > 30 ns (Fig. 1), also in combination with predefined phase dependencies between multiple generators, the plasma temperature can be optimally controlled and a non-thermal equilibrium plasma can be generated.
All these technological developments are certainly associated with additional costs. The start-up investment in semiconductor technologies is currently still higher than for the well-established magnetrons. Whereas with magnetrons there is no further potential for savings in comparison to SSPG's. But due to the very long-life expectancy of the generators, which is currently well above 100.000 hours, compared to the 3.000 to 8.000 hours of the magnetrons., it is still profitable within few years (Fig. 2). Thereby is ensured a reliable and stable process and in combination with the modularity and suitably dimensioned redundant power, ensure an uninterrupted operation.

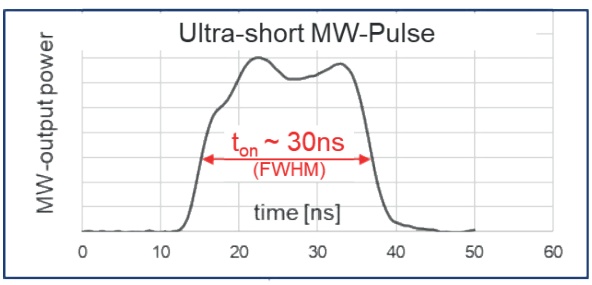

Figure 1 *Ultra-short microwave pulses*

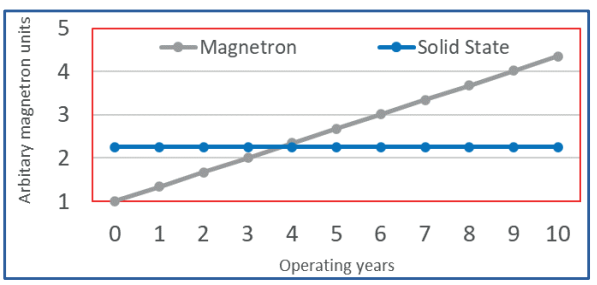

Figure 2 *Cost comparison 6-kW Magnetron/SolidState*

Poster 19

Advanced modeling of melt turbulence, impurities and bubble transport in Cz silicon crystal growth

Vladimir Artemyev[1], Andrey Smirnov[1]

Semiconductor Technology Research d.o.o. Beograd

e-mail: Vladimir.Artemyev@str-soft.com

Silicon monocrystals are widely used in different industrial applications such as microcircuits, solar cells, power electronics. For obtaining high quality monocrystals it is necessary to control the melt flow, concentration of impurities and bubbles, which incorporate into the crystal during the growth process. The imposed transversal or cusp magnetic fields are commonly used to control the transport of impurities and bubbles by turbulent melt flow and for stabilizing the growth process. Present work demonstrates new and unique physical models and approaches implemented in the latest version of CGSim software package for analysis of the problems announced.

Due to high melt temperature which hinders experimental investigation of turbulent melt convection, numerical simulation is a promising way for obtaining information about the distributions of velocity and temperature as well as concentrations of different impurities and mechanisms of bubble transport inside the melt. Nowadays the most popular approaches for modeling of turbulence are RANS and RANS/LES. Both approaches necessitate a turbulence model to be applied for the calculation of the turbulent effective viscosity. However, the eddy viscosity models do not capture the anisotropy of heat and mass transport in the melt which is especially important in the vicinity of the free surface. Due to above-mentioned limitations of eddy viscosity models, STR *k* model which accounts for the anisotropy effects by using GGDH (Generalized Gradient Diffusion Hypothesis) for modeling the turbulent heat and mass fluxes and STR (Stress Tensor Reconstruction) assumption for modeling the Reynolds stress tensor [2-3] has been used. Accounting for the anisotropy of Reynolds stresses help to reproduce the turbulent kinetic energy (TKE) shear production term which acts as both source and sink terms. We present a comparison of the results obtained using STR *k* model with a reference implicit LES computation and conventional eddy viscosity model.

Pin-holes is one of defects observed in Cz silicon crystals for electronics and may be the reason of monocrystalline structure loss, and reduce product yield from the wafer [4]. The nature of pin-holes are bubbles, which are generated at the inner crucible boundary, transported by the melt flow and buoyancy forces towards the melt/crystal interface, and incorporate into the growing crystal [5]. Bubble transport is mostly governed by the melt flow, which structure might be very complex, especially in case of using horizontal magnetic fields. To reveal mechanisms responsible for bubble transport in different conditions, and perform process optimization to reduce bubble incorporation, the bubble transport model has been developed and implemented in CGSim software package. Modeling results together with analysis of bubble transport of different diameter for 300 mm Cz silicon growth will be presented.

[1] R. Yokoyama, T. Nakamura, W. Sugimura, T. Ono, T. Fujiwara, K. Kakimoto, Time-dependent behavior of melt flow in the industrial scale silicon Czochralski growth with a transverse magnetic field, J. Cryst. Growth 519 (2019) 77-83.

[2] V. Kalaev, D. Borisov, A. Smirnov, A modified hypothesis of Reynolds stress tensor modeling for mixed turbulent convection in crystal growth, J. Cryst. Growth 580 (2022) 126464, https://doi.org/10.1016/j.jcrysgro.2021.126464.

[3] D. Borisov, V. Artemyev, V. Kalaev, A. Smirnov, A. Kuliev, F. Zobel, R. Kunert, R. Turan, O. Aydin, I. Kabacelik, Advanced approach for oxygen transport and crystallization front calculation in Cz silicon crystal growth, J. Cryst. Growth 583 (2022) 126493, https://doi.org/10.1016/j.jcrysgro.2021.126493.

[4] A. Lanterne, G. Gaspar, Y. Hu, E. Øvrelid, M. Di Sabatino, Characterization of the loss of the dislocation-free growth during Czochralski silicon pulling, J. Cryst. Growth Volume 458 (2017) 120-128.

[5] J. Paloheimo: Properties of silicon crystals, in Handbook of Silicon Based MEMS Materials and Technologies, V. Lindroos, M. Tilli, A. Lehto, T. Motooka (Eds.), first ed., William Andrew Publishing, 2010, ISBN 978-0-8155-1594-4, p. 50. https://doi.org/10.1016/B978-0-44-453153-7.00089-4.

Digital Defect Traceability across Sapphire Processing: Case Study on Micro-LED Chain

Dr. Ivan Orlov,[1] Dr. Gourav Sen,[2] Dr. Caroline Chèze,[1] and Frédéric Falise[1]
[1]*Scientific Visual, Lausanne, Switzerland,*
[2]*Fametec-Ebner GmbH, Leonding, Austria,*
welcome@scientificvisual.ch

LEDs and micro-LEDs industries crucially depend on the sapphire substrate: 96.7% of the global LED production in 2020 was achieved on sapphire wafers (see https://www.cryscore.com/technical-info/). Material defects in the substrates - such as micro-bubbles, clouds, and structures - cause rejection of finished wafers and may also disrupt large production lines for weeks. Sapphire core suppliers mitigate this risk by imposing increasingly stringent quality requirements on their production and scrap a considerable part of fresh-grown sapphire, even though it can be used if adequately evaluated.

This project is to help sapphire manufacturers to transition to digital quality control that leads to material saving by:

- Tracing how defects in raw sapphire crystals affect the quality of micro-LED wafers,
- Identifying critical defect features that decrease the wafer yield,
- Coding-relevant indicators into the raw crystal scanner software,
- Increasing productivity by 'intelligent wafering', i.e., proactively improving wafer processing through computer-aided optimization.

This contribution presents preliminary results of tracing yield-impacting material defects through crystal processing stages (Fig.1). For this study, the Fametec-Ebner sapphire unit has grown 96 *c*-axis Ø7" HEM crystals. The material was produced in several furnaces to reduce the effect of random fluctuations. Five 7" rough crystals were chosen out of the 96 to represent the full range of quality, from clean to very defective and with a substantial variability of defect morphology and size, and to be processed into 6-inch cores. Authors underline that the chosen highly flawed crystals do not represent the quality of Fametec-Ebner production.

The crystals were scanned at all processing stages at the TotalScan™ scanner operated by Scientific Visual in Lausanne, Switzerland. The scanning system automatically detects bubbles down to 10 µm, structures, and clouds in raw crystals of any shape. In parallel, the defectiveness was assessed by experts using manual methods to compare the reliability of human and automated TotalScan™ defect identification at every stage.

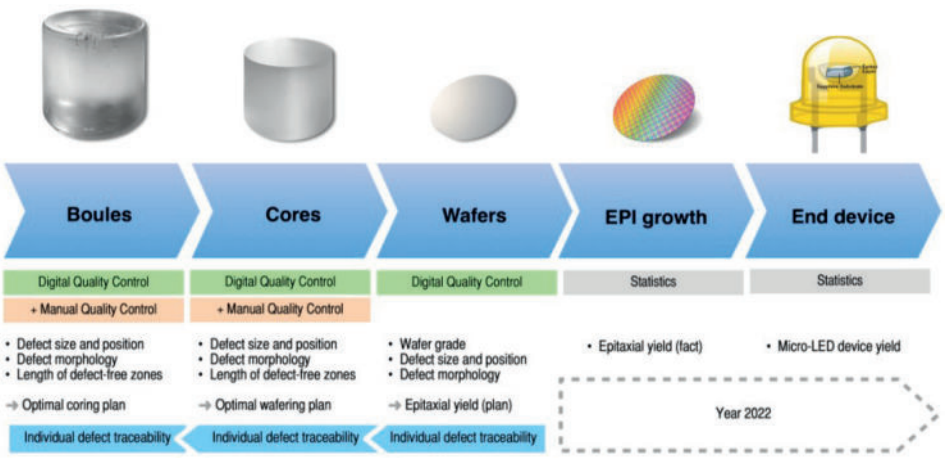

Fig.1. End-to-End study design.

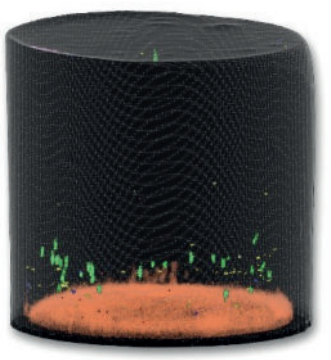

Fig 2. 3D model showing a defect pattern in one of the 7" raw HEM crystals used in the test. Color code corresponds to different defect types.

After wafering the core, each wafer was analyzed using an automated KLA-Tencor Candela® system, which indicated whether it was compliant with the micro-LED specification.

The 3D defect patterns data (Fig. 2) from each processing stage were integrated using the *Scientific Visual Yield Pro v4.4* software. Such reconstruction allowed tracing individual defects in sapphire as they passed through consecutive production stages: raw crystals (boules) ➜ cores ➜ EPI-ready wafers.

We correlated defects yield-impacting in polished wafers with the ones identified by TotalScan™ in the raw crystals thanks to end-to-end defect tracing. The correlations confirmed that the digitalization of crystal quality control offers tangible opportunities for processing companies to extract more quality wafers, save resources, and improve their profitability. In particular, we show that digital quality control increases wafer yield from 5 to 20% by *intelligent wafering*, i.e., by correctly positioning the sapphire core in a wafering system.

Acknowledgments: The authors acknowledge the project support by the Eurostars and the Innosuisse – Swiss Innovation Agency.

Leibniz-Institut für Kristallzüchtung (IKZ)
im Forschungsverbund Berlin e.V.

Max-Born-Str. 2, 12489 Berlin
Tel.: +49 (0)30 6392-3001
Fax: +49 (0)30 9392-3003
Email: iwcgt-8@ikz-berlin.de
www.ikz-berlin.de

Bildnachweis:

Kristallbilder: IKZ
Berlin-Silhouette: clker.com Free Clipart
Stadtplan: OpenStreetMap

IWCGT-8 | Schedule

Time	Sun 29, May	Mon, 30 May	Tue, 31 May	Wed, 1 June	Thu, 2 June
08:50am		Zaidat	Xu (online)	Dropka	Jeandel
09:50am		Krahnert	Rudolph	Stockmeier	Li
10:40am		Coffee	Coffee	Coffee	Coffee
11:10am		Menzel	Otoki (online)	Hell	Mühe
12:00pm		Break	Break	Hikavyy	Closing
12:30pm		Lunch	Lunch		Lunch
12:50pm				Lunch	
02:10pm		Furukawa	Wegener	Break (SC Meeting)	
03:00pm		Tremsin (online)	Dalmau (online)		
03:50pm		Coffee	Coffee	Excursion (Boat tour)	
04:30pm	Registration	Havlíček	Eichler		
05:20pm	Welcome	Sen	Raghavan		
06:10pm		Break	Break	Gala Dinner	
06:30pm	Dinner	Dinner	Dinner		
07:30pm	Get together	Poster1	Poster2		
08:00pm	Panel				
09:30pm	End	End	End		